Supplementary Material for "Nonreciprocal Ground-State Cooling of Multiple Mechanical Resonators"

Deng-Gao Lai,[1,2] Jin-Feng Huang,[1] Xian-Li Yin,[1] Bang-Pin Hou,[3] Wenlin Li,[4] David Vitali,[4,5,6] Franco Nori,[2,7] and Jie-Qiao Liao[1,*]

[1]*Key Laboratory of Low-Dimensional Quantum Structures and Quantum Control of Ministry of Education, Key Laboratory for Matter Microstructure and Function of Hunan Province, Department of Physics and Synergetic Innovation Center for Quantum Effects and Applications, Hunan Normal University, Changsha 410081, China*

[2]*Theoretical Quantum Physics Laboratory, RIKEN, Saitama 351-0198, Japan*

[3]*College of Physics and Electronic Engineering, Institute of Solid State Physics, Sichuan Normal University, Chengdu 610068, China*

[4]*School of Science and Technology, Physics Division, University of Camerino, Camerino (MC), Italy*

[5]*INFN, Sezione di Perugia, I-06123 Perugia, Italy*

[6]*CNR-INO, L.go Enrico Fermi 6, I-50125 Firenze, Italy*

[7]*Physics Department, The University of Michigan, Ann Arbor, Michigan 48109-1040, USA*

(Dated: April 17, 2020)

PACS numbers:

This document consists of ten parts: (I) The dark-mode effect and its breaking in a two-mechanical-resonator optomechanical system; (II) Ground-state cooling of the two mechanical resonators; (III) Phonon scattering probability and nonreciprocal phonon transfer; (IV) Derivation of the cooling limits of the two mechanical resonators; (V) Analyzing the dark-mode effect and breaking the dark-mode effect in a multi-mechanical-resonator optomechanical system; (VI) Ground-state cooling of the multiple mechanical resonators; (VII) Discussions on the justification of performing the rotating-wave approximation (RWA); (VIII) Simultaneous cooling of the mechanical supermodes; (IX) Physical mechanism for breaking the dark-state effect in a Lambda-type three-level system; (X) A possible experimental realization and derivation of a phase-dependent phonon-hopping interaction between two mechanical resonators.

I. THE DARK-MODE EFFECT AND ITS BREAKING IN A TWO-MECHANICAL-RESONATOR OPTOMECHANICAL SYSTEM

In this section, we analyze the dark-mode effect in a two-mechanical-resonator optomechanical system, which is composed of one cavity-field mode and two mechanical resonators. Note that here we only consider one mechanical mode in each mechanical resonator. We also show that the dark-mode effect can be broken by introducing a phase-dependent phonon-exchange interaction between the two mechanical resonators. In a rotating frame defined by the transform operator $\exp(-i\omega_L t a^\dagger a)$, the total Hamiltonian of the system reads ($\hbar = 1$)

$$H_I = \Delta_c a^\dagger a + \omega_1 b_1^\dagger b_1 + \omega_2 b_2^\dagger b_2 + g_1 a^\dagger a(b_1 + b_1^\dagger) + g_2 a^\dagger a(b_2 + b_2^\dagger) + (\Omega a + \Omega^* a^\dagger) + \eta(e^{i\theta} b_1^\dagger b_2 + e^{-i\theta} b_2^\dagger b_1), \quad \text{(S1)}$$

where $\Delta_c = \omega_c - \omega_L$ is the detuning of the cavity-field resonance frequency ω_c with respect to the cavity-field driving frequency ω_L. The operators a ($a^\dagger$) and $b_{l=1,2}$ ($b_l^\dagger$) are, respectively, the annihilation (creation) operators of the cavity-field mode and the lth mechanical resonator, with the corresponding resonance frequencies ω_c and ω_l. The g_1 and g_2 terms in Hamiltonian (S1) describe the optomechanical coupling between the cavity mode and the lth mechanical resonator, with $g_{l=1,2}$ being the single-photon optomechanical-coupling strength. The Ω term denotes the cavity-field driving with the driving amplitude Ω. To control the energy exchange between the two mechanical resonators, we introduce a phase-dependent phonon-exchange interaction between the two mechanical resonators, with the coupling strength η and the phase θ.

According to Hamiltonian (S1), the Langevin equations for the annihilation operators of the optical and mechanical modes can be obtained by phenologically adding the dissipation and noise terms into the Heisenberg equations of

*Electronic address: jqliao@hunnu.edu.cn

motion as

$$\dot{a} = -\{\kappa + i[\Delta_c + g_1(b_1 + b_1^\dagger) + g_2(b_2 + b_2^\dagger)]\}a - i\Omega^* + \sqrt{2\kappa}a_{\rm in}, \tag{S2a}$$

$$\dot{b}_1 = -(\gamma_1 + i\omega_1)b_1 - ig_1 a^\dagger a - i\eta e^{i\theta}b_2 + \sqrt{2\gamma_1}b_{1,\rm in}, \tag{S2b}$$

$$\dot{b}_2 = -(\gamma_2 + i\omega_2)b_2 - ig_2 a^\dagger a - i\eta e^{-i\theta}b_1 + \sqrt{2\gamma_2}b_{2,\rm in}, \tag{S2c}$$

where κ and $\gamma_{l=1,2}$ are the decay rates of the cavity-field mode and the lth mechanical resonator, respectively. The operators $a_{\rm in}$ and $b_{l=1,2,\rm in}$ ($a_{\rm in}^\dagger$ and $b_{l,\rm in}^\dagger$) are the noise operators associated with the cavity-field mode and the lth mechanical resonator, respectively. These noise operators have zero mean values and the following correlation functions,

$$\langle a_{\rm in}(t)a_{\rm in}^\dagger(t')\rangle = \delta(t-t'), \tag{S3a}$$

$$\langle a_{\rm in}^\dagger(t)a_{\rm in}(t')\rangle = 0, \tag{S3b}$$

$$\langle b_{l,\rm in}(t)b_{l,\rm in}^\dagger(t')\rangle = (\bar{n}_l + 1)\delta(t-t'), \tag{S3c}$$

$$\langle b_{l,\rm in}^\dagger(t)b_{l,\rm in}(t')\rangle = \bar{n}_l\delta(t-t'), \tag{S3d}$$

where $\bar{n}_{l=1,2}$ is the average thermal-phonon occupation number associated with the heat bath of the lth mechanical resonator. In this paper we consider a vacuum bath for the cavity field and a heat bath (with $\bar{n}_{l=1,2}$) for each mechanical resonator. The vacuum bath of the cavity field provides the cooling reservoir to absorb the thermal excitations extracted from the two mechanical resonators.

To cool the mechanical resonators, we consider the strong-driving regime of the cavity such that the average photon number in the cavity is sufficiently large and then the linearization procedure can be used to simplify the physical model. To this end, we expand the quantum fluctuations of the system around their steady-state values and express the operators in Eq. (S2) as a summation of their steady-state mean values and quantum fluctuations, namely $o = \langle o\rangle_{\rm ss} + \delta o$ for operators $o = a$, $a^\dagger$, $b_{l=1,2}$, and $b_{l=1,2}^\dagger$. By separating the classical motion and quantum fluctuations, the linearized equations of motion for quantum fluctuations can be written as

$$\delta\dot{a} = -(\kappa + i\Delta)\delta a - iG_1(\delta b_1 + \delta b_1^\dagger) - iG_2(\delta b_2 + \delta b_2^\dagger) + \sqrt{2\kappa}a_{\rm in}, \tag{S4a}$$

$$\delta\dot{b}_1 = -iG_1^*\delta a - (\gamma_1 + i\omega_1)\delta b_1 - i\eta e^{i\theta}\delta b_2 - iG_1\delta a^\dagger + \sqrt{2\gamma_1}b_{1,\rm in}, \tag{S4b}$$

$$\delta\dot{b}_2 = -iG_2^*\delta a - i\eta e^{-i\theta}\delta b_1 - (\gamma_2 + i\omega_2)\delta b_2 - iG_2\delta a^\dagger + \sqrt{2\gamma_2}b_{2,\rm in}, \tag{S4c}$$

where $\Delta = \Delta_c + 2(g_1{\rm Re}[\beta_1] + g_2{\rm Re}[\beta_2])$ is the normalized driving detuning of the cavity field with ${\rm Re}[\beta_l]$ extracting the real part of β_l, and $G_{l=1,2} = g_l\alpha$ is the strength of the linearized optomechanical coupling between the cavity field and the lth mechanical resonator. Here, the steady-state solutions of the classical motion (namely the steady-state average values of the operators of the system) can be obtained as

$$\alpha \equiv \langle a\rangle_{\rm ss} = \frac{-i\Omega^*}{\kappa + i\Delta}, \tag{S5a}$$

$$\beta_1 \equiv \langle b_1\rangle_{\rm ss} = \frac{-i\left(g_1|\alpha|^2 + \eta e^{i\theta}\beta_2\right)}{\gamma_1 + i\omega_1}, \tag{S5b}$$

$$\beta_2 \equiv \langle b_2\rangle_{\rm ss} = \frac{-i\left(g_2|\alpha|^2 + \eta e^{-i\theta}\beta_1\right)}{\gamma_2 + i\omega_2}. \tag{S5c}$$

For simplicity, in the following discussions we consider the case where α is real, which is accessible by choosing a proper driving amplitude Ω. Then the linearized optomechanical coupling strengths G_1 and G_2 are real.

A linearized optomechanical Hamiltonian can be inferred according to Eqs. (S4). For studying quantum cooling of the two mechanical resonators, the beam-splitting-type interactions (i.e., the rotating-wave interaction term) between these bosonic modes are expected to dominate the linearized couplings in this system, and hence we can simplify the Hamiltonian of the system by making the rotating-wave approximation (RWA). The linearized optomechanical Hamiltonian in the RWA takes the following form (discarding the noise terms)

$$H_{\rm RWA} = \Delta\delta a^\dagger\delta a + \omega_1\delta b_1^\dagger\delta b_1 + \omega_2\delta b_2^\dagger\delta b_2 + G_1(\delta a\delta b_1^\dagger + \delta b_1\delta a^\dagger) + G_2(\delta a\delta b_2^\dagger + \delta b_2\delta a^\dagger) + \eta(e^{i\theta}\delta b_1^\dagger\delta b_2 + e^{-i\theta}\delta b_2^\dagger\delta b_1), \tag{S6}$$

where δa ($\delta a^\dagger$) and $\delta b_{l=1,2}$ ($\delta b_l^\dagger$) are the fluctuation operators of the cavity-field mode and the lth mechanical resonator, respectively.

To see the dark-mode effect in this two-mechanical-resonator optomechanical system, we first consider the case where the phase-dependent phonon-exchange interaction between the two mechanical resonators is absent, i.e., $\eta = 0$. In this case, the coupled two-mechanical-mode system forms two hybrid mechanical modes: a bright mode and a dark mode, which are expressed by the new annihilation operators as

$$B_+ = \frac{1}{\sqrt{G_1^2 + G_2^2}}(G_1\delta b_1 + G_2\delta b_2), \tag{S7a}$$

$$B_- = \frac{1}{\sqrt{G_1^2 + G_2^2}}(G_2\delta b_1 - G_1\delta b_2). \tag{S7b}$$

These new operators satisfy the bosonic commutation relations $[B_+, B_+^\dagger] = 1$ and $[B_-, B_-^\dagger] = 1$. In the absence of the phonon-exchange interaction ($\eta = 0$), the Hamiltonian in Eq. (S6) can be rewritten with the two hybrid modes as

$$H_{\rm hyb} = \Delta\delta a^\dagger\delta a + \omega_+ B_+^\dagger B_+ + \omega_- B_-^\dagger B_- + \zeta(B_+^\dagger B_- + B_-^\dagger B_+) + G_+(\delta a B_+^\dagger + B_+\delta a^\dagger), \tag{S8}$$

where we introduce the resonance frequencies $\omega_\pm$ and the coupling strengths ζ and G_+

$$\omega_+ = \frac{G_1^2\omega_1 + G_2^2\omega_2}{G_1^2 + G_2^2}, \tag{S9a}$$

$$\omega_- = \frac{G_2^2\omega_1 + G_1^2\omega_2}{G_1^2 + G_2^2}, \tag{S9b}$$

$$\zeta = \frac{G_1G_2(\omega_1 - \omega_2)}{G_1^2 + G_2^2}, \tag{S9c}$$

$$G_+ = \sqrt{G_1^2 + G_2^2}. \tag{S9d}$$

When $\omega_1 = \omega_2$, the two hybrid modes are decoupled from each other due to $\zeta = 0$, and the mode B_- becomes a dark mode in the sense that it is decoupled from both the cavity mode a and the other hybrid mode B_+.

In order to break the dark-mode effect, we introduce a phase-dependent phonon-exchange interaction (i.e., the η term) between the two mechanical resonators. By introducing two new bosonic modes $\tilde{B}_+$ and $\tilde{B}_-$ defined by

$$\delta b_1 = f\tilde{B}_+ + e^{i\theta}h\tilde{B}_-, \tag{S10a}$$

$$\delta b_2 = -e^{-i\theta}h\tilde{B}_+ + f\tilde{B}_-, \tag{S10b}$$

Hamiltonian (S6) becomes

$$H_{\rm RWA} = \Delta\delta a^\dagger\delta a + \tilde{\omega}_+\tilde{B}_+^\dagger\tilde{B}_+ + \tilde{\omega}_-\tilde{B}_-^\dagger\tilde{B}_- + (\tilde{G}_+^*\delta a\tilde{B}_+^\dagger + \tilde{G}_+\tilde{B}_+\delta a^\dagger) + (\tilde{G}_-^*\delta a\tilde{B}_-^\dagger + \tilde{G}_-\tilde{B}_-\delta a^\dagger), \tag{S11}$$

where we introduce the resonance frequencies $\tilde{\omega}_\pm$ and the coupling strengths $\tilde{G}_\pm$ as

$$\tilde{\omega}_\pm = \frac{1}{2}(\omega_1 + \omega_2 \pm \sqrt{(\omega_1 - \omega_2)^2 + 4\eta^2}), \tag{S12a}$$

$$\tilde{G}_+ = fG_1 - e^{-i\theta}hG_2, \tag{S12b}$$

$$\tilde{G}_- = e^{i\theta}hG_1 + fG_2, \tag{S12c}$$

with

$$f = \frac{|\tilde{\omega}_- - \omega_1|}{\sqrt{(\tilde{\omega}_- - \omega_1)^2 + \eta^2}}, \tag{S13a}$$

$$h = \frac{\eta f}{\tilde{\omega}_- - \omega_1}. \tag{S13b}$$

In the degenerate-resonator case, namely when the two mechanical resonators have the same resonance frequencies $\omega_1 = \omega_2 = \omega_m$, the coupling strengths in Eq. (S12) can be simplified as

$$\tilde{G}_+ = (G_1 + e^{-i\theta}G_2)/\sqrt{2}, \tag{S14a}$$

$$\tilde{G}_- = (G_2 - e^{i\theta}G_1)/\sqrt{2}. \tag{S14b}$$

We proceed to analyze the dependence of the dark-mode effect on the coupling strengths G_1 and G_2. Concretely, we will consider three special cases.

(i) In the symmetric-coupling case: $G_1 = G_2 = G$, we obtain the relations

$$\tilde{G}_+ = G(1 + e^{-i\theta})/\sqrt{2}, \tag{S15a}$$
$$\tilde{G}_- = G(1 - e^{i\theta})/\sqrt{2}. \tag{S15b}$$

It can be seen from Eq. (S15) that, when $\theta = n\pi$ for an integer n, one of the two hybrid mechanical modes (the dark mode) will be decoupled from the cavity-field mode. In this case, the excitation energy stored in the dark mode cannot be extracted through the optomechanical-cooling channel. In general cases of $\theta \neq n\pi$, the dark-mode effect is broken and then ground-state cooling of the two mechanical resonators becomes accessible under proper parameter conditions.

(ii) In the case $\theta = n\pi$ for an even number n, Eq. (S14) becomes

$$\tilde{G}_+ = (G_1 + G_2)/\sqrt{2}, \tag{S16a}$$
$$\tilde{G}_- = (G_2 - G_1)/\sqrt{2}. \tag{S16b}$$

We can see that the dark mode (i.e., the mode $\tilde{B}_-$ in this case) can be broken when the two optomechanical coupling strengths are different $G_1 \neq G_2$. In this case, our numerical simulation indicates that simultaneous ground-state cooing of the two mechanical resonators can be realized when $G_2/G_1 \ll 1$.

(iii) In the case $\theta = n\pi$ for an odd number n, we have

$$\tilde{G}_+ = (G_1 - G_2)/\sqrt{2}, \tag{S17a}$$
$$\tilde{G}_- = (G_2 + G_1)/\sqrt{2}. \tag{S17b}$$

In this case, the mode $\tilde{B}_+$ becomes the dark mode when $G_1 = G_2$. The simultaneous ground-state cooing of the two mechanical resonators can be realized when $G_2/G_1 \ll 1$, as shown by Fig. S2(d).

II. GROUND-STATE COOLING OF THE TWO MECHANICAL RESONATORS

In this section, we study the cooling performance in this system by evaluating the final average phonon numbers in the two mechanical resonators. To this end, we proceed to rewrite the linearized Langevin equations (S4) as the following compact form

$$\dot{\mathbf{u}}(t) = \mathbf{A}\mathbf{u}(t) + \mathbf{N}(t), \tag{S18}$$

where the fluctuation operator vector $\mathbf{u}(t)$, the noise operator vector $\mathbf{N}(t)$, and the coefficient matrix $\mathbf{A}$ are defined as

$$\mathbf{u}(t) = [\delta a(t), \delta b_1(t), \delta b_2(t), \delta a^\dagger(t), \delta b_1^\dagger(t), \delta b_2^\dagger(t)]^T, \tag{S19}$$

$$\mathbf{N}(t) = [\sqrt{2\kappa}a_{\rm in}(t), \sqrt{2\gamma_1}b_{1,\rm in}(t), \sqrt{2\gamma_2}b_{2,\rm in}(t), \sqrt{2\kappa}a_{\rm in}^\dagger(t), \sqrt{2\gamma_1}b_{1,\rm in}^\dagger(t), \sqrt{2\gamma_2}b_{2,\rm in}^\dagger(t)]^T, \tag{S20}$$

and

$$\mathbf{A} = \begin{pmatrix} -(\kappa + i\Delta) & -iG_1 & -iG_2 & 0 & -iG_1 & -iG_2 \\ -iG_1^* & -(\gamma_1 + i\omega_1) & -i\eta e^{i\theta} & -iG_1 & 0 & 0 \\ -iG_2^* & -i\eta e^{-i\theta} & -(\gamma_2 + i\omega_2) & -iG_2 & 0 & 0 \\ 0 & iG_1^* & iG_2^* & -(\kappa - i\Delta) & iG_1^* & iG_2^* \\ iG_1^* & 0 & 0 & iG_1 & -(\gamma_1 - i\omega_1) & i\eta e^{-i\theta} \\ iG_2^* & 0 & 0 & iG_2 & i\eta e^{i\theta} & -(\gamma_2 - i\omega_2) \end{pmatrix}. \tag{S21}$$

The formal solution of the linearized Langevin equation (S18) can be written as

$$\mathbf{u}(t) = \mathbf{M}(t)\mathbf{u}(0) + \int_0^t \mathbf{M}(t-s)\mathbf{N}(s)ds, \tag{S22}$$

where the matrix $\mathbf{M}(t)$ is defined by $\mathbf{M}(t) = \exp(\mathbf{A}t)$. Based on the solution, we can calculate the steady-state average phonon numbers in the two mechanical resonators by solving the Lyapunov equation. Note that the parameters used in the following calculations satisfy the stability conditions derived from the Routh-Hurwitz criterion. Namely, the real parts of all the eigenvalues of the coefficient matrix $\mathbf{A}$ are negative.

For studying quantum cooling of the two mechanical resonators, we focus on the final average phonon numbers in the two mechanical resonators by calculating the steady-state value of the covariance matrix $\mathbf{V}$, which is defined by the matrix elements

$$\mathbf{V}_{ij} = \frac{1}{2}[\langle \mathbf{u}_i(\infty)\mathbf{u}_j(\infty)\rangle + \langle \mathbf{u}_j(\infty)\mathbf{u}_i(\infty)\rangle], \qquad i,j = 1-6. \tag{S23}$$

In the linearized optomechanical system, the covariance matrix $\mathbf{V}$ satisfies the Lyapunov equation

$$\mathbf{A}\mathbf{V} + \mathbf{V}\mathbf{A}^T = -\mathbf{Q}, \tag{S24}$$

where "T" denotes the matrix transpose operation and the matrix $\mathbf{Q}$ is defined by

$$\mathbf{Q} = \frac{1}{2}(\mathbf{C} + \mathbf{C}^T), \tag{S25}$$

with $\mathbf{C}$ being the noise correlation matrix defined by the matrix elements

$$\langle \mathbf{N}_k(s)\mathbf{N}_l(s')\rangle = \mathbf{C}_{k,l}\delta(s-s'). \tag{S26}$$

For the Markovian baths considered in this work, the constant matrix $\mathbf{C}$ is given by

$$\mathbf{C} = \begin{pmatrix} 0 & 0 & 0 & 2\kappa & 0 & 0 \\ 0 & 0 & 0 & 0 & 2\gamma_1(\bar{n}_1+1) & 0 \\ 0 & 0 & 0 & 0 & 0 & 2\gamma_2(\bar{n}_2+1) \\ 0 & 0 & 0 & 0 & 0 & 0 \\ 0 & 2\gamma_1\bar{n}_1 & 0 & 0 & 0 & 0 \\ 0 & 0 & 2\gamma_2\bar{n}_2 & 0 & 0 & 0 \end{pmatrix}. \tag{S27}$$

Based on the covariance matrix $\mathbf{V}$, the final average phonon numbers in the two mechanical resonators are obtained by

$$n_1^f = \langle \delta b_1^\dagger \delta b_1\rangle = \mathbf{V}_{52} - \frac{1}{2}, \tag{S28a}$$

$$n_2^f = \langle \delta b_2^\dagger \delta b_2\rangle = \mathbf{V}_{63} - \frac{1}{2}, \tag{S28b}$$

where $\mathbf{V}_{52}$ and $\mathbf{V}_{63}$ can be obtained by solving the Lyapunov equation (S24).

In Figs. S1(a) and S1(b), we plot the final average phonon numbers n_1^f and n_2^f as functions of the ratio ω_2/ω_1 (the resonance frequency of the second mechanical resonator over that of the first mechanical resonator) and the scaled cavity-field decay rate κ/ω_1 when the phase-dependent phonon-exchange coupling is absent ($\eta = 0$), i.e., in the dark-mode-unbreaking case. Here, we can see that there exists a peak around $\omega_2 = \omega_1$, which means that the two mechanical resonators cannot be cooled in the degenerate and near-degenerate two-resonator cases. This phenomenon can be clearly explained based on the dark-mode effect. When $\omega_1 = \omega_2$, the two mechanical resonators form two hybrid mechanical modes: a bright mode and a dark mode. The dark mode is decoupled from both the cavity-field mode and the bright mechanical mode and hence the excitation energy stored in the dark mode cannot be extracted through the optomechanical-cooling channel. When the two mechanical resonators are far-off-resonant with each other, there is no dark mode, then the ground-state cooling can be realized when this system works in the resolved-sideband regime and under proper driving condition (red-sideband resonance).

The dark-mode effect can be broken by introducing a phase-dependent phonon-exchange interaction between the two mechanical resonators, and then the ground-state cooling can be realized in the degenerate and near-degenerate two-mechanical-resonator cases. In Figs. S1(c) and S1(d), we plot the final average phonon numbers n_1^f and n_2^f in the two mechanical resonators as functions of the ratio ω_2/ω_1 and the scaled cavity-field decay rate κ/ω_1 in the dark-mode-breaking case ($\eta/\omega_1 = 0.05$ and $\theta = \pi/2$). Different from the results in Figs. S1(a) and S1(b), here we can see that the simutaneous ground-state cooling can be realized ($n_{1,2}^f \ll 1$) in the resolved-sideband regime ($\kappa \ll \omega_1$), which is consistent with the sideband-cooling results in a typical optomechanical system. In addition, simultaneous ground-state cooling of the two mechanical resonators can be reached in a wide parameter range of ω_2/ω_1. We also

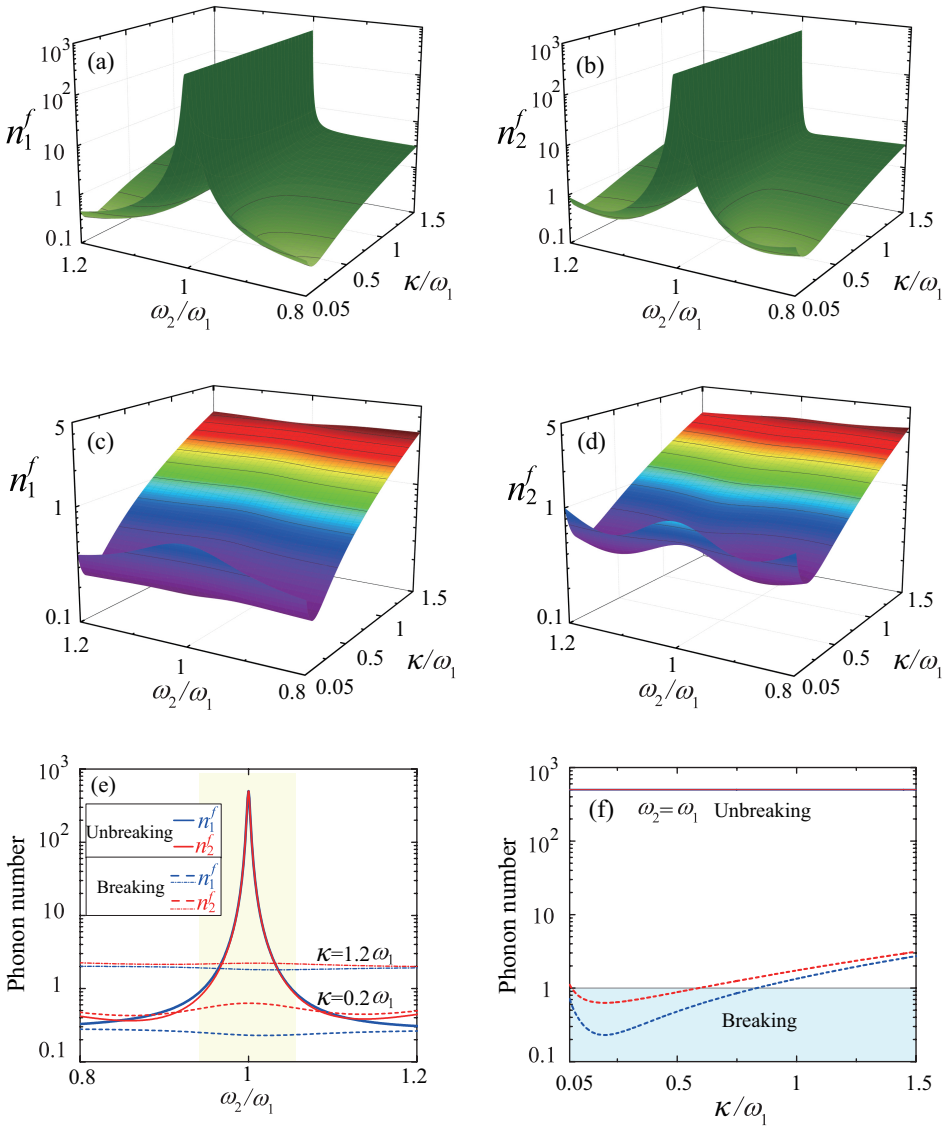

FIG. S1: (Color online) The final average phonon numbers n_1^f and n_2^f versus the resonance-frequency ratio ω_2/ω_1 and the cavity-field decay rate κ scaled by ω_1 in both (a,b) the dark-mode-unbreaking case ($\eta/\omega_1 = 0$) and (c,d) the dark-mode-breaking case ($\eta/\omega_1 = 0.05$ and $\theta = \pi/2$). (e) The final average phonon numbers n_1^f (blue curves) and n_2^f (red curves) as functions of ω_2/ω_1 in both the dark-mode-unbreaking case ($\eta/\omega_1 = 0$, solid curves) and the dark-mode-breaking case ($\eta/\omega_1 = 0.05$ and $\theta = \pi/2$, dashed curves) under either $\kappa/\omega_1 = 0.2$ or $\kappa/\omega_1 = 1.2$. (f) The final average phonon numbers n_1^f (blue curves) and n_2^f (red curves) versus κ/ω_1 in both the dark-mode-unbreaking case ($\eta/\omega_1 = 0$, solid curves) and the dark-mode-breaking case ($\eta/\omega_1 = 0.05$ and $\theta = \pi/2$, dashed curves) when $\omega_1 = \omega_2$. Here, we consider red-sideband resonance driving $\Delta = \omega_1$. Other used parameters are given by $G_1/\omega_1 = G_2/\omega_1 = 0.1$, $\gamma_1/\omega_1 = \gamma_2/\omega_1 = 10^{-5}$, and $\bar{n}_1 = \bar{n}_2 = 10^3$.

see that the cooling performance of the first resonator is better than that of the second resonator ($n_1^f < n_2^f$). This is because the phase $\theta = \pi/2$ is chosen in this case. As we will see in the following section, the nonreciprocal phonon transfer is more helpful to cool the first (second) resonator when $0 < \theta < \pi$ ($\pi < \theta < 2\pi$).

We note that though the dark mode exists theoretically only in the degenerate-resonator case of this optomechanical system, i.e., $\omega_1 = \omega_2$, the dark-mode effect works within a finite parameter range of the near-degenerate-resonator case. To know the width of the frequency-detuning window associated with the dark-mode effect, in Fig. S1(e) we show the final average phonon numbers n_1^f and n_2^f as functions of the ratio ω_2/ω_1 in both the dark-mode-unbreaking ($\eta/\omega_1 = 0$) and -breaking ($\eta/\omega_1 = 0.05$ and $\theta = \pi/2$) cases. For the dark-mode-unbreaking case, the ground-state cooling cannot be reached in the degenerate and near-degenerate-resonator cases, as marked by the shadow area. The width of the shadow area can be characterized by the effective mechanical linewidth ($\Delta\omega = |\omega_2 - \omega_1| \leq \Gamma_l = \gamma_l + \gamma_{l,\mathrm{opt}}$). This is because the cooling of the two mechanical resonators is suppressed in this region, i.e., the two mechanical

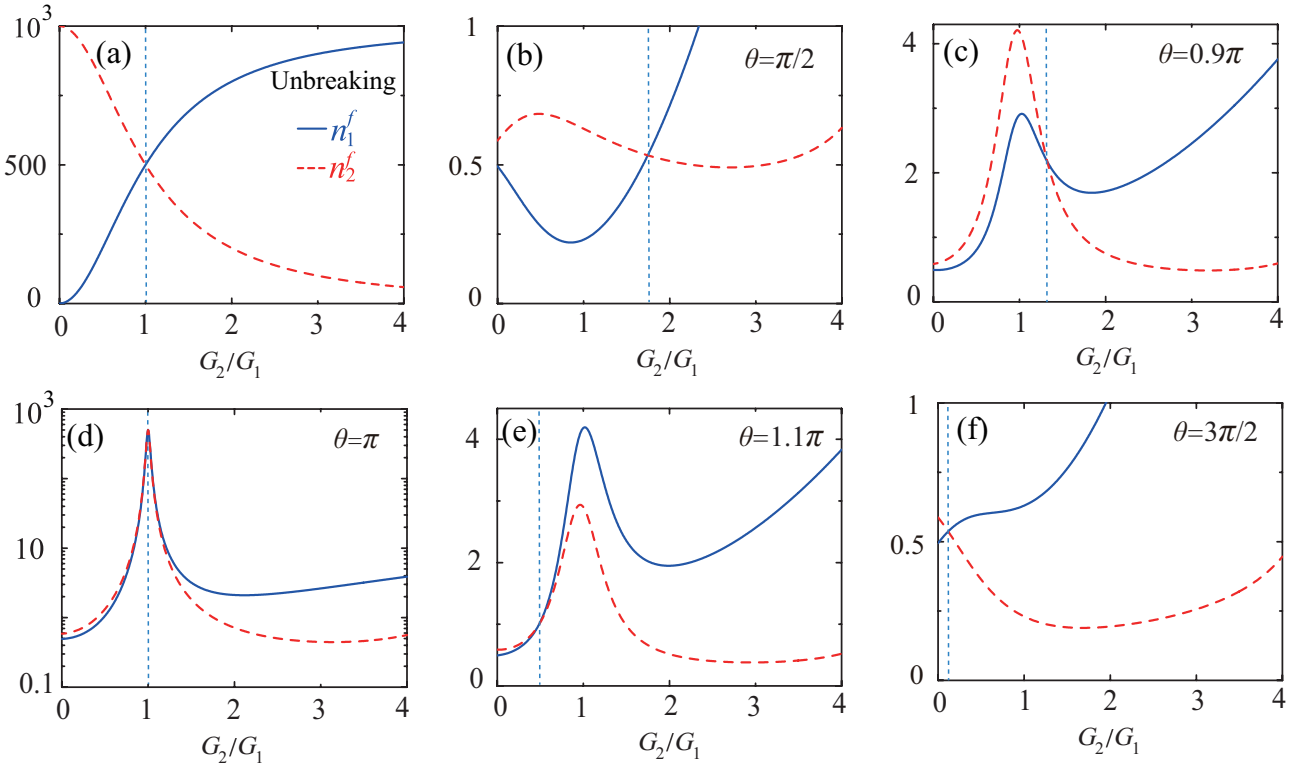

FIG. S2: (Color online) The final average phonon numbers n_1^f (blue solid curves) and n_2^f (red dashed curves) as functions of the ratio G_2/G_1 when the phonon-exchange coupling parameters θ and η take various values: (a) $\eta/\omega_1 = 0$, (b-f) $\eta/\omega_1 = 0.05$ and $\theta = \pi/2$, 0.9π, π, 1.1π, and $3\pi/2$. Here we choose the optimal driving $\Delta = \omega_1 = \omega_2 = \omega_m$, $\kappa/\omega_m = 0.2$, $G_1/\omega_m = 0.1$, $\gamma_1/\omega_m = \gamma_2/\omega_m = 10^{-5}$, and $\bar{n}_1 = \bar{n}_2 = 10^3$.

resonators have significant spectral overlap and become effectively degenerate. In the dark-mode-breaking case, we can see that the ground-state cooling can be realized irrespective of the value of the ratio ω_2/ω_1 in the resolved-sideband regime ($\kappa/\omega_1 = 0.2$). When the phonon sidebands cannot be resolved, the ground-state cooling is unaccessible in this system (see the curves corresponding to $\kappa/\omega_1 = 1.2$). Especially, in this shadow area shown in Fig. S1(e), the emergences of a small valley (the blue dashed curve) and a small hill (the red dashed curve) can be explained based on the nonreciprocical phonon transfer. At an optimal nonreciprocical phonon-transfer point ($\omega_1 = \omega_2$, $\theta = \pi/2$), the phonons in the first mechanical resonator are extracted through both the optomechanical-cooling channel and the phonon-exchange channel, while the phonons in the second mechanical resonator are extracted only through the optomechanical-cooling channel. This is because the phonon transmission rate from modes b_2 (b_1) to b_1 (b_2) is zero (a finite value) in this case.

We also investigate the influence of the cavity-field decay rate κ on the cooling efficiency in both the dark-mode-breaking and -unbreaking cases. In Fig. S1(f), we plot the final average phonon numbers n_1^f and n_2^f as functions of the scaled cavity-field decay rate κ/ω_1 in both the dark-mode-unbreaking and -breaking cases when the two mechanical resonators have the same resonance frequencies $\omega_1 = \omega_2$. Here, we can see that, in the dark-mode-unbreaking case, the final phonon numbers n_1^f and n_2^f are approximately 500. This is because the energy (half of the thermal phonons) stored in the dark mode cannot be extracted and hence the mechanical resonators cannot be cooled. In the dark-mode-breaking case, the ground-state cooling can be reached when the system works in the resolved-sideband regime. The optimal working parameter of the cavity-field decay rate (corresponding to the minimal value of the final mean phonon numbers) is around $\kappa/\omega_1 \approx 0.2$. This optimal value is reached under the combined competition between the optomechanical-cooling rate (i.e., the excitation-energy extraction efficiency through the cavity-field decay channel) and the phonon-sideband resolution condition.

In the above discussions concerning Fig. S1, we only consider the symmetric-coupling case, i.e., $G_1 = G_2$. To better understand quantum cooling in this system, we also investigate the dependence of the final average phonon numbers n_1^f and n_2^f on the linearized optomechanical-coupling strengths G_1 and G_2. In Fig. S2, we plot the final average phonon numbers n_1^f and n_2^f as functions of the ratio G_2/G_1 when the phonon-exchange coupling parameters η and θ take various values: (a) $\eta/\omega_m = 0$, (b-f) $\eta/\omega_m = 0.05$ and $\theta = \pi/2$, 0.9π, π, 1.1π, and $3\pi/2$. When the phonon-

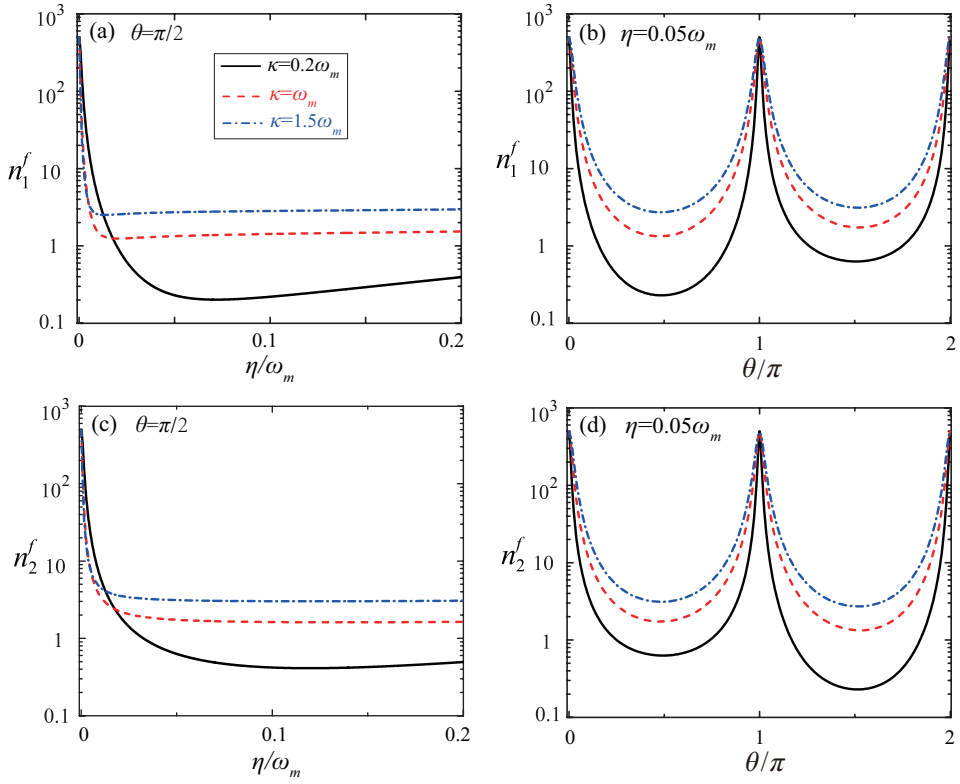

FIG. S3: (Color online) The final average phonon numbers (a,c) n_1^f and (b,d) n_2^f versus either (a,b) the coupling strength η at $\theta = \pi/2$ or (c,d) the phase θ at $\eta = 0.05\omega_m$ when the cavity-field decay rate takes various values: $\kappa/\omega_m = 0.2$, 1, and 1.5. Here we choose $\Delta = \omega_1 = \omega_2 = \omega_m$, $G_1/\omega_m = G_2/\omega_m = 0.1$, $\gamma_1/\omega_m = \gamma_2/\omega_m = 10^{-5}$, and $\bar{n}_1 = \bar{n}_2 = 10^3$.

exchange coupling is absent, i.e., $\eta = 0$ [Fig. S2(a)], the final average phonon number in the first (second) mechanical resonator increases (decreases) with the increase of G_2/G_1. However, we point out that, due to the dark-mode effect, the ground-state cooling of the two mechanical resonators are unfeasible for finite values of the ratio G_2/G_1. When $G_2/G_1 < 1$, the bright mechanical mode is dominated by mode b_1. When $G_2/G_1 > 1$, the bright mechanical mode is dominated by mode b_2. As a result, the cooling efficiency of the first mechanical resonator is better (worse) than that of the second one in the parameter range $G_2/G_1 < 1$ ($G_2/G_1 > 1$). The cooling performance of the two resonators is exchanged when the value of the ratio G_2/G_1 changes across the point $G_2/G_1 = 1$. In the symmetric-coupling case $G_2/G_1 = 1$, the same cooling performance is achieved for the two mechanical resonators ($n_1^f = n_2^f \approx 500$). The physical reason is that the optomechanical-cooling channels for the two mechanical resonators take the same role when $G_1 = G_2$. At this point, the superposition amplitudes of the two mechanical modes b_1 and b_2 in the bright and dark modes are the same, as shown in Eq. (S7b). In the presence of the phonon-exchange coupling, the ground-state cooling can be realized in a wide parameter range of the ansymmetric couplings $G_2 \neq G_1$ when $\theta \neq n\pi$ for integer n. In addition, we can see a similar intersection phenomenon for the cooling performance of the two resonators with the increase of the ratio G_2/G_1. However, the location of the intersection point moves to the right (left) from the point $G_2/G_1 = 1$ when the phase θ takes the value in the range $0 < \theta < \pi$ ($\pi < \theta < 2\pi$). This shift is caused by the phase-dependent phonon-exchange coupling between the two mechanical resonators. When $0 < \theta < \pi$, the phonon-exchange coupling assists the cooling of the first mechanical resonator (i.e., decreasing n_1^f and increasing n_2^f). Hence the phonon-exchange coupling pushes the intersection point moving right. When $\pi < \theta < 2\pi$, the phonon-exchange coupling assists the cooling of the second mechanical resonator (i.e., decreasing n_2^f and increasing n_1^f). As a result, the phonon-exchange coupling pushes the intersection point moving left. At $\theta = \pi$ [panel (d)], the dark mode appears in this system when $G_1 = G_2$, then the two mechanical modes cannot be cooled. In this case, the dark-mode effect can be broken by choosing different values of the coupling strengths $G_1 \neq G_2$, i.e., simultaneous ground-state cooling of the two mechanical resonators can only be realized when $G_2/G_1 \leq 0.5$.

The phase-dependent phonon-exchange interaction plays a critical role in the ground-state cooling of the multiple mechanical resonators. Below we investigate the dependence of the cooling performance on the coupling parameters η and θ of the phase-dependent phonon-exchange interaction between the two mechanical resonators. In Figs. S3(a)

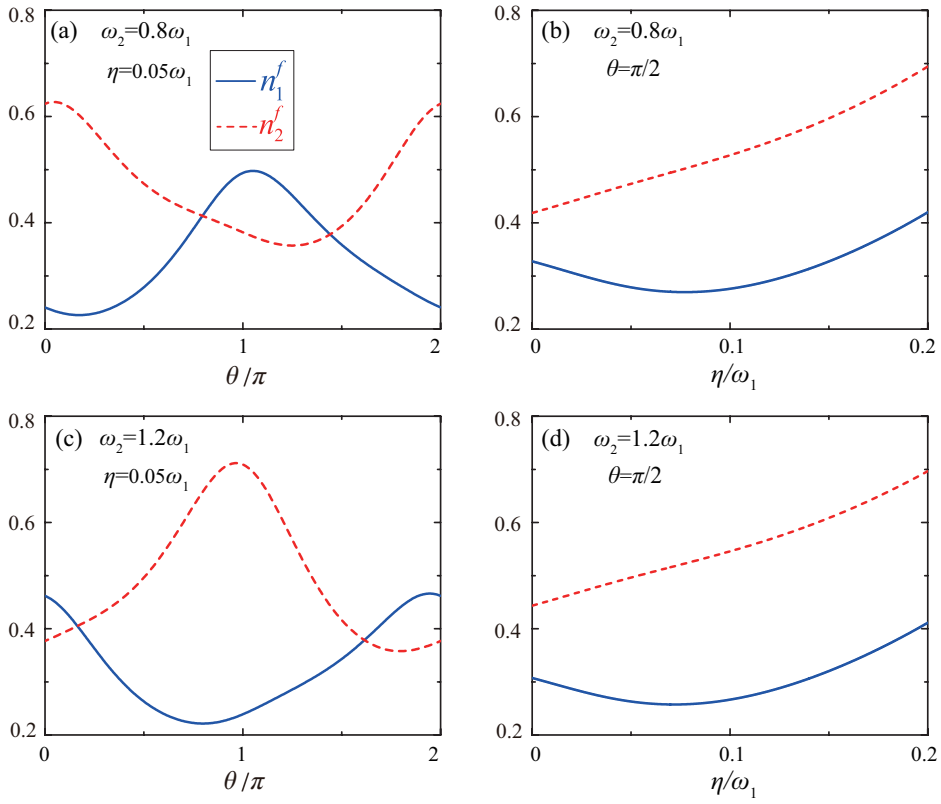

FIG. S4: (Color online) The final average phonon numbers n_1^f (blue solid curves) and n_2^f (red dashed curves) versus the phase θ and the phonon-exchange coupling strength η in the nondegenerate two-resonator cases (a,b) $\omega_2 = 0.8\omega_1$ and (c,d) $\omega_2 = 1.2\omega_1$. Here we choose $\Delta = \omega_1$, $G_1/\omega_1 = G_2/\omega_1 = 0.1$, $\kappa/\omega_1 = 0.2$, $\gamma_1/\omega_1 = \gamma_2/\omega_1 = 10^{-5}$, and $\bar{n}_1 = \bar{n}_2 = 10^3$.

and S3(b), we plot the final average phonon numbers n_1^f and n_2^f as functions of the coupling strength η and phase θ when the cavity-field decay rate takes various values: $\kappa/\omega_m = 0.2$, 1, and 1.5. Here, we can see that the two mechanical resonators can be cooled efficiently (from the initial phonon number 1000 to the final phonon number below 10) when $\eta/\omega_m > 0.02$. In addition, the cooling performance becomes worse for a larger value of the cavity-field decay rate κ. The ground-state cooling can only be realized in the resolved-sideband regime $\kappa/\omega_m < 1$. We also show the dependence of the final average phonon numbers n_1^f and n_2^f on the phase θ for several values of κ/ω_m, as shown in Figs. S3(c) and S3(d). The plots show that the cooling performance depends on the phase θ. The final average phonon numbers n_1^f and n_2^f can be largely decreased when $0 < \theta < \pi$ and $\pi < \theta < 2\pi$. When $\theta = n\pi$ for an integer n, the two mechanical resonators cannot be cooled due to the dark-mode effect. The cooling performance becomes worse with the increase of the cavity-field decay rate. In addition, the results show that $n_1^f < n_2^f$ ($n_1^f > n_2^f$) in the parameter range $0 < \theta < \pi$ ($\pi < \theta < 2\pi$), which can be explained based on the nonreciprocal phonon transfer induced by quantum interference in the loop-coupled system.

In Fig. S3, we have investigated the dependence of the final average phonon numbers n_1^f and n_2^f on the phonon-exchange coupling parameters η and θ in the degenerate two-mechanical-resonator case, i.e., $\omega_1 = \omega_2$. In the following we also consider a nondegenerate mechanical-resonator case. In Fig. S4 we plot the final average phonon numbers n_1^f and n_2^f versus the parameters η and θ in the nondegenerate two-resonator cases, i.e., $\omega_2 = 0.8\omega_1$ or $\omega_2 = 1.2\omega_1$. The plots show that the simultaneous ground-state cooling of the two mechanical resonators can be realized in the nondegenerate mechanical-resonator case. In both the cases $\omega_2 = 0.8\omega_1$ and $\omega_2 = 1.2\omega_1$, the dependence of n_1^f and n_2^f on the phase θ has an inverse tendency, as shown in Figs. S4(a) and S4(c). In addition, the dependence of $n_{l=1,2}^f$ on the phase θ in the case $\omega_2 = 0.8\omega_1$ is inverse to that in the case of $\omega_2 = 1.2\omega_1$. In Figs. S4(b) and S4(d), we can see $n_1^f < n_2^f$ and the dependence of $n_{l=1,2}^f$ on the coupling strength η has a similar tendency for the cases $\omega_2 = 0.8\omega_1$ and $\omega_2 = 1.2\omega_1$. In the nondegenerate-resonator case, the cooling performance can be controlled by choosing proper phonon-exchange coupling parameters η and θ. The same value of the final phonon numbers n_1^f and n_2^f can be obtained by choosing the intersection points in Figs. S4(a) and S4(c).

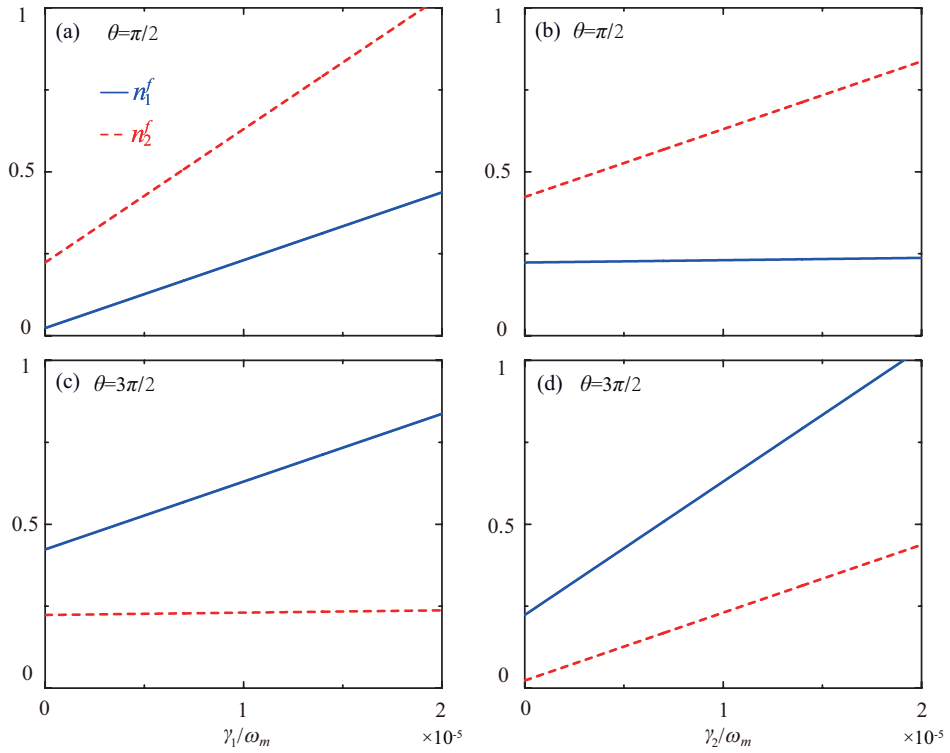

FIG. S5: (Color online) The final average phonon numbers n_1^f and n_2^f as functions of (a,c) γ_1 and (b,d) γ_2 when the phase θ takes different values: (a,b) $\theta = \pi/2$ and (c,d) $\theta = 3\pi/2$. In panels (a,c) and (b,d), we choose $\gamma_2/\omega_1 = 10^{-5}$ and $\gamma_1/\omega_1 = 10^{-5}$, respectively. Other used parameters are $\Delta = \omega_1 = \omega_2 = \omega_m$, $G_1/\omega_m = G_2/\omega_m = 0.1$, $\eta/\omega_m = 0.05$, $\kappa/\omega_m = 0.2$, and $\bar{n}_1 = \bar{n}_2 = 10^3$.

In quantum cooling of the mechanical resonators, the optomechanical cavity and its vacuum bath provide the cooling channel to extract the excitation energy in the mechanical resonators. Here, the mechanical resonators are thermalized by their thermal baths through the mechanical dissipation channels. As a result, the final average phonon numbers n_1^f and n_2^f in the two mechanical resonators depend on the mechanical decay rates γ_1 and γ_2. In Fig. S5, we show the final average phonon numbers n_1^f and n_2^f as functions of the decay rates γ_1 and γ_2. We can see that n_1^f and n_2^f increase with the increase of the mechanical decay rates. This is because the energy exchange rates between the mechanical resonators and their heat baths are faster for larger values of the decay rates, and then the thermal excitation in the heat baths will raise the total phonon numbers in the mechanical resonators. In Figs. S5(a) and S5(b), we have $n_1^f < n_2^f$ because the phase angle $\theta = \pi/2$ is taken, then the cooling performance of the first resonator is better than that of the second resonator. However, an opposite cooling effect compared with the case of $\theta = \pi/2$ emerges when $\theta = 3\pi/2$, as shown in Figs. S5(c) and S5(d). These interesting cooling phenomena can be explained according to the phonon scattering process between the two mechanical resonators, which will be studied in the next section.

III. PHONON SCATTERING PROBABILITY AND NONRECIPROCAL PHONON TRANSFER

In this section, we study the scattering probabilities of the phonon transport between the two mechanical resonators coupled by a phase-dependent phonon-exchange interaction. We calculate the transmission spectrum of the phonon transport based on the Langevin equation (S18). To this end, we rewrite the matrix $\mathbf{N}(t)$ defined in Eq. (S20) as

$$\mathbf{N}(t) = \mathbf{\Gamma}\mathbf{u}_{\rm in}(t), \tag{S29}$$

where the damping matrix $\mathbf{\Gamma}$ is defined as

$$\mathbf{\Gamma} = \mathbf{diag}[\sqrt{2\kappa}, \sqrt{2\gamma_1}, \sqrt{2\gamma_2}, \sqrt{2\kappa}, \sqrt{2\gamma_1}, \sqrt{2\gamma_2}], \tag{S30}$$

with **diag**$[x]$ giving a matrix with the elements of the list x on the leading diagonal, and 0 elsewhere. The input noise vector $\mathbf{u}_{\rm in}(t)$ in Eq. (S29) is given by

$$\mathbf{u}_{\rm in}(t) = [a_{\rm in}(t), b_{1,\rm in}(t), b_{2,\rm in}(t), a^\dagger_{\rm in}(t), b^\dagger_{1,\rm in}(t), b^\dagger_{2,\rm in}(t)]^T. \tag{S31}$$

Making use of the Fourier transformation for operator $r \in \{\delta a, \delta b_1, \delta b_2, \delta a_{\rm in}, \delta b_{1,\rm in}, \delta b_{2,\rm in}\}$ and its conjugate $r^\dagger$,

$$\tilde{r}(\omega) = \frac{1}{2\pi}\int_{-\infty}^{\infty} e^{i\omega t} r(t) dt, \tag{S32a}$$

$$\tilde{r}^\dagger(\omega) = \frac{1}{2\pi}\int_{-\infty}^{\infty} e^{i\omega t} r^\dagger(t) dt, \tag{S32b}$$

the solutions to the linearized quantum Langevin equation (S18) in the frequency domain can be obtained as

$$\tilde{\mathbf{u}}(\omega) = (-i\omega\mathbf{I} - \mathbf{A})^{-1}\mathbf{\Gamma}\tilde{\mathbf{u}}_{\rm in}(\omega), \tag{S33}$$

where $\tilde{\mathbf{u}}(\omega)$ and $\tilde{\mathbf{u}}_{\rm in}(\omega)$ are, respectively, the Fourier transformation of the operator vectors $\mathbf{u}(t)$ defined in Eq. (S19) and $\mathbf{u}_{\rm in}(t)$ defined in Eq. (S31). The matrix $\mathbf{I}$ in Eq. (S33) is an identity matrix. Using the input-output relation

$$o_{\rm in} + o_{\rm out} = \sqrt{2\gamma_o}\delta o \tag{S34}$$

for $o \in \{a, b_1, b_2\}$ and $\gamma_o \in \{\kappa, \gamma_1, \gamma_2\}$, we obtain the output field in the frequency domain as

$$\tilde{\mathbf{u}}_{\rm out}(\omega) = \mathbf{U}(\omega)\tilde{\mathbf{u}}_{\rm in}(\omega), \tag{S35}$$

where the transformation matrix is given by

$$\mathbf{U}(\omega) = \mathbf{\Gamma}(-i\omega\mathbf{I} - \mathbf{A})^{-1}\mathbf{\Gamma} - \mathbf{I}, \tag{S36}$$

and

$$\tilde{\mathbf{u}}_{\rm out}(\omega) = [\tilde{a}_{\rm out}(\omega), \tilde{b}_{1,\rm out}(\omega), \tilde{b}_{2,\rm out}(\omega), \tilde{a}^\dagger_{\rm out}(\omega), \tilde{b}^\dagger_{1,\rm out}(\omega), \tilde{b}^\dagger_{2,\rm out}(\omega)]^T \tag{S37}$$

denotes the Fourier transformation of $\mathbf{u}_{\rm out}(t)$.

To analyze the excitation energy transfer in this system, we introduce the spectra for the input and output signals as

$$\mathbf{S}_{\rm in}(\omega) = [s_{a,\rm in}(\omega), s_{b_1,\rm in}(\omega), s_{b_2,\rm in}(\omega)]^T, \tag{S38a}$$

$$\mathbf{S}_{\rm out}(\omega) = [s_{a,\rm out}(\omega), s_{b_1,\rm out}(\omega), s_{b_2,\rm out}(\omega)]^T, \tag{S38b}$$

where the elements are defined by

$$\langle\tilde{o}^\dagger_{\rm out}(\omega')\tilde{o}_{\rm out}(\omega)\rangle = s_{o,\rm out}\delta(\omega+\omega'), \tag{S39a}$$

$$\langle\tilde{o}^\dagger_{\rm in}(\omega')\tilde{o}_{\rm in}(\omega)\rangle = s_{o,\rm in}\delta(\omega+\omega'), \tag{S39b}$$

$$\langle\tilde{o}_{\rm in}(\omega')\tilde{o}^\dagger_{\rm in}(\omega)\rangle = (1+s_{o,\rm in})\delta(\omega+\omega'). \tag{S39c}$$

We also define the spectrum for the input vacuum noise as

$$\mathbf{S}_{\rm vac}(\omega) = [s_{a,\rm vac}(\omega), s_{b_1,\rm vac}(\omega), s_{b_2,\rm vac}(\omega)]^T, \tag{S40}$$

with

$$s_{a,\rm vac}(\omega) = |U_{14}(\omega)|^2 + |U_{15}(\omega)|^2 + |U_{16}(\omega)|^2, \tag{S41a}$$

$$s_{b_1,\rm vac}(\omega) = |U_{24}(\omega)|^2 + |U_{25}(\omega)|^2 + |U_{26}(\omega)|^2, \tag{S41b}$$

$$s_{b_2,\rm vac}(\omega) = |U_{34}(\omega)|^2 + |U_{35}(\omega)|^2 + |U_{36}(\omega)|^2. \tag{S41c}$$

Then the relation between these spectra can be obtained as

$$\mathbf{S}_{\rm out}(\omega) = \mathbf{T}(\omega)\mathbf{S}_{\rm in}(\omega) + \mathbf{S}_{\rm vac}(\omega), \tag{S42}$$

where the transmission matrix $\mathbf{T}(\omega)$ is defined by

$$\mathbf{T}(\omega)=\begin{pmatrix} T_{aa}(\omega) & T_{ab_1}(\omega) & T_{ab_2}(\omega) \\ T_{b_1a}(\omega) & T_{b_1b_1}(\omega) & T_{b_1b_2}(\omega) \\ T_{b_2a}(\omega) & T_{b_2b_1}(\omega) & T_{b_2b_2}(\omega) \end{pmatrix}, \tag{S43}$$

with these matrix elements

$$\begin{aligned} T_{aa}(\omega) &= |U_{11}(\omega)|^2+|U_{14}(\omega)|^2, \\ T_{ab_1}(\omega) &= |U_{12}(\omega)|^2+|U_{15}(\omega)|^2, \\ T_{ab_2}(\omega) &= |U_{13}(\omega)|^2+|U_{16}(\omega)|^2, \\ T_{b_1a}(\omega) &= |U_{21}(\omega)|^2+|U_{24}(\omega)|^2, \\ T_{b_1b_1}(\omega) &= |U_{22}(\omega)|^2+|U_{25}(\omega)|^2, \\ T_{b_1b_2}(\omega) &= |U_{23}(\omega)|^2+|U_{26}(\omega)|^2, \\ T_{b_2a}(\omega) &= |U_{31}(\omega)|^2+|U_{34}(\omega)|^2, \\ T_{b_2b_1}(\omega) &= |U_{32}(\omega)|^2+|U_{35}(\omega)|^2, \\ T_{b_2b_2}(\omega) &= |U_{33}(\omega)|^2+|U_{36}(\omega)|^2. \end{aligned} \tag{S44}$$

The element $T_{vw}(\omega)$ ($v,w\in\{a,b_1,b_2\}$) denotes the transmittance from the input mode w to the output mode v. To explore the phonon-transfer nonreciprocity between the two mechanical modes, we only focus on the transmittance $T_{b_1b_2}(\omega)$ and $T_{b_2b_1}(\omega)$ between the two mechanical modes. Then, we numerically evaluate the transmittance between the two mechanical modes to show the nonreciprocal phonon transfer. Physically, the transmittance $T_{b_1b_2}(\omega)$ and $T_{b_2b_1}(\omega)$ can be used to analyze the thermal excitations extracted from one mechanical mode to the other one.

The above results concerning the phonon transmission are exact. Below we derive some approximate analytical results under the RWA and the resonance condition $\Delta=\omega_1=\omega_2=\omega_m$. Note that under the RWA, we have the approximate relations $T_{b_1b_2}(\omega)\approx|U_{23}(\omega)|^2$ and $T_{b_2b_1}(\omega)\approx|U_{32}(\omega)|^2$. In particular, we focus on the resonant phonon transmission at the mechanical frequency ω_m, then an analytical transmittance between the two mechanical modes can be obtained as

$$\begin{aligned} T_{b_1b_2}\approx&|U_{23}|^2=\frac{4\gamma_1\gamma_2[(G_1G_2)^2+(\kappa\eta)^2-2G_1G_2\kappa\eta\sin\theta]}{(G_2^2\gamma_1+G_1^2\gamma_2+\kappa\gamma_1\gamma_2+\kappa\eta^2)^2+4(G_1G_2\eta\cos\theta)^2} \\ =&\frac{4(\mathcal{C}_1\mathcal{C}_2+\mathcal{C}_3-2\sqrt{\mathcal{C}_1\mathcal{C}_2\mathcal{C}_3}\sin\theta)}{(\mathcal{C}_1+\mathcal{C}_2+\mathcal{C}_3+1)^2+4\mathcal{C}_1\mathcal{C}_2\mathcal{C}_3\cos^2\theta}, \end{aligned} \tag{S45a}$$

$$\begin{aligned} T_{b_2b_1}\approx&|U_{32}|^2=\frac{4\gamma_1\gamma_2[(G_1G_2)^2+(\kappa\eta)^2+2G_1G_2\kappa\eta\sin\theta]}{(G_2^2\gamma_1+G_1^2\gamma_2+\kappa\gamma_1\gamma_2+\kappa\eta^2)^2+4(G_1G_2\eta\cos\theta)^2} \\ =&\frac{4(\mathcal{C}_1\mathcal{C}_2+\mathcal{C}_3+2\sqrt{\mathcal{C}_1\mathcal{C}_2\mathcal{C}_3}\sin\theta)}{(\mathcal{C}_1+\mathcal{C}_2+\mathcal{C}_3+1)^2+4\mathcal{C}_1\mathcal{C}_2\mathcal{C}_3\cos^2\theta}, \end{aligned} \tag{S45b}$$

where we introduce the cooperativities between any two subsystems in this two-mechanical-mode optomechanical system as

$$\mathcal{C}_1=\frac{G_1^2}{\gamma_1\kappa}, \tag{S46a}$$

$$\mathcal{C}_2=\frac{G_2^2}{\gamma_2\kappa}, \tag{S46b}$$

$$\mathcal{C}_3=\frac{\eta^2}{\gamma_1\gamma_2}. \tag{S46c}$$

According to Eqs. (S45a) and (S45b), the maximum transmittance for either $\theta=\pi/2$ or $\theta=3\pi/2$ can be obtained as

$$(T_{b_2b_1})_{\max}=(T_{b_1b_2})_{\max}=\frac{4(\sqrt{\mathcal{C}_1\mathcal{C}_2}+\sqrt{\mathcal{C}_3})^2}{(\mathcal{C}_1+\mathcal{C}_2+\mathcal{C}_3+1)^2}. \tag{S47}$$

By introducing a relative phonon-scattering rate from the mechanical modes w to v as

$$\Lambda_{vw}=\frac{T_{vw}-T_{wv}}{(T_{vw})_{\max}}, \tag{S48}$$

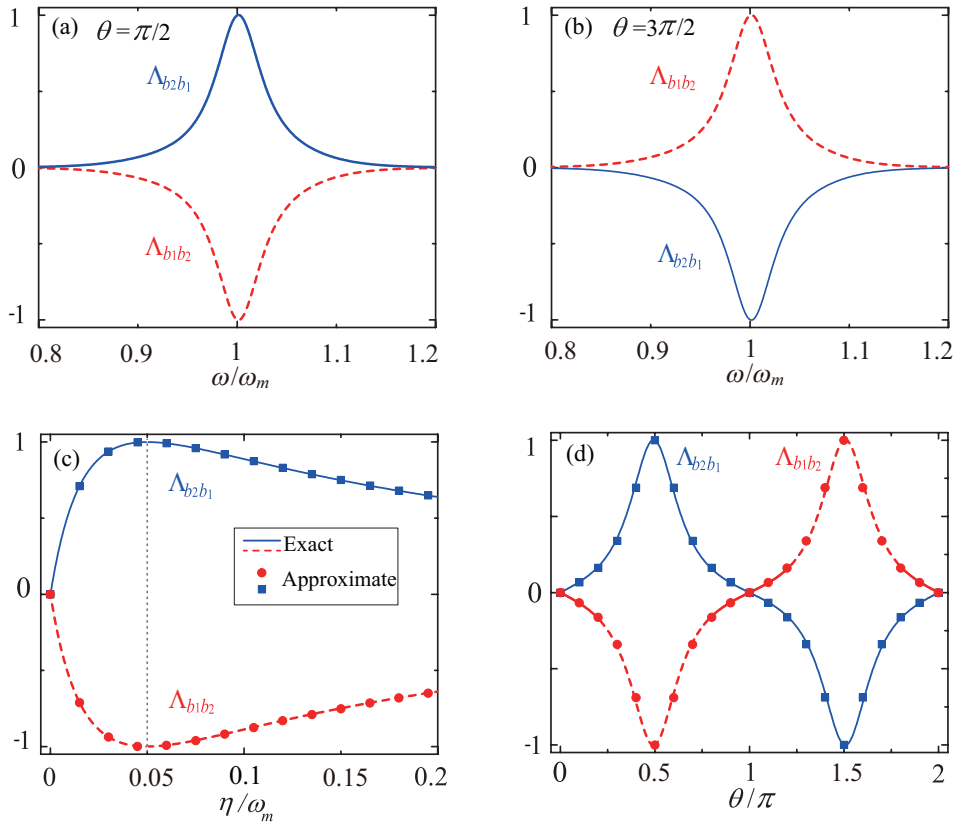

FIG. S6: (Color online) (a,b) The relative phonon-scattering rate $\Lambda_{b_2b_1}$ (blue curves) and $\Lambda_{b_1b_2}$ (red curves) as functions of ω when the phase θ takes different values: (a) $\theta=\pi/2$ and (b) $\theta=3\pi/2$. In panels (a,b), we choose the phonon-exchange coupling $\eta/\omega_m=0.05$. (c,d) The exact (solid/dashed lines) and approximate (symbols) relative resonant-phonon-scattering rates $\Lambda_{b_2b_1}$ and $\Lambda_{b_1b_2}$ vs (c) the phonon-exchange coupling η when $\theta=\pi/2$ and (d) the phase θ when $\eta/\omega_m=0.05$ under the parameter $\omega=\omega_m$. Here we take $\Delta=\omega_1=\omega_2=\omega_m$, $G_1/\omega_m=G_2/\omega_m=0.1$, $\kappa/\omega_m=0.2$, $\gamma_1/\omega_m=\gamma_2/\omega_m=10^{-5}$, and $\bar{n}_1=\bar{n}_2=10^3$.

we can then obtain the rates between the two mechanical modes b_1 and b_2 as

$$\Lambda_{b_2b_1}=\frac{T_{b_2b_1}-T_{b_1b_2}}{(T_{b_2b_1})_{\max}}=\frac{4\sqrt{\mathcal{C}_1\mathcal{C}_2\mathcal{C}_3}\sin\theta}{(\sqrt{\mathcal{C}_1\mathcal{C}_2}+\sqrt{\mathcal{C}_3})^2\left(1+\frac{4\mathcal{C}_1\mathcal{C}_2\mathcal{C}_3\cos^2\theta}{(\mathcal{C}_1+\mathcal{C}_2+\mathcal{C}_3+1)^2}\right)}, \tag{S49a}$$

$$\Lambda_{b_1b_2}=\frac{T_{b_1b_2}-T_{b_2b_1}}{(T_{b_1b_2})_{\max}}=-\Lambda_{b_2b_1}. \tag{S49b}$$

In Figs. S6(a) and S6(b), the relative phonon-scattering rates $\Lambda_{b_2b_1}$ (blue curves) and $\Lambda_{b_1b_2}$ (red curves) are plotted as functions of the scaled frequency ω/ω_m when the phase θ takes different values: (a) $\theta=\pi/2$ and (b) $\theta=3\pi/2$. It is obviously shown that the reciprocity of the phonon transfer between the two mechanical resonators is broken ($\Lambda_{b_2b_1}\neq 0$) in a wide range of ω and the phonon transfer exhibits a perfect nonreciprocal response when $\theta=\pi/2$ and $\theta=3\pi/2$. When $\theta=\pi/2$ ($\theta=3\pi/2$), we have $T_{b_2b_1}>0$ and $T_{b_1b_2}<0$ ($T_{b_2b_1}<0$ and $T_{b_1b_2}>0$). In particular, when $\omega=\omega_m$ and $\theta=\pi/2$, we have $\Lambda_{b_2b_1}=1$, i.e., $T_{b_1b_2}=0$. This means that the unidirectional flow of the phonons from b_1 to b_2 is achieved. When $\omega=\omega_m$ and $\theta=3\pi/2$, we have $\Lambda_{b_1b_2}=1$, i.e., $T_{b_2b_1}=0$. This means the phonons can only be transferred from b_2 to b_1. Based on the above results, we can see that the phase-dependent phonon-exchange coupling plays an effective role on the relative phonon scattering between the two mechanical resonators. In Figs. S6(c) and S6(d), we show the dependence of the relative resonant-phonon-scattering rates on the phonon-exchange coupling parameters η and θ. The results indicate that a perfect nonreciprocal phonon transfer requires both $\eta\approx 0.05\omega_m$ and $\theta=\pi/2$ or $3\pi/2$. Moreover, the exact calculations and the approximate analytical results match well with each other. Here, the solid ($\Lambda_{b_2b_1}$) and dashed lines ($\Lambda_{b_1b_2}$) are plotted using the exact solutions, while the symbols are based on the analytical calculations given in Eqs. (S49a) and (S49b). In Fig. S6(d), when $0<\theta<\pi$, it shows $\Lambda_{b_2b_1}>0$, i.e., $T_{b_2b_1}>T_{b_1b_2}$. In the region $\pi<\theta<2\pi$, it exhibits $\Lambda_{b_1b_2}>0$, i.e., $T_{b_1b_2}>T_{b_2b_1}$. Meanwhile, the phonon transmission satisfies the reciprocity [$\Lambda_{b_2b_1}=\Lambda_{b_1b_2}=0$, i.e., $T_{b_1b_2}=T_{b_2b_1}$] at $\theta=n\pi$. Moreover, the transmittance is optimal for

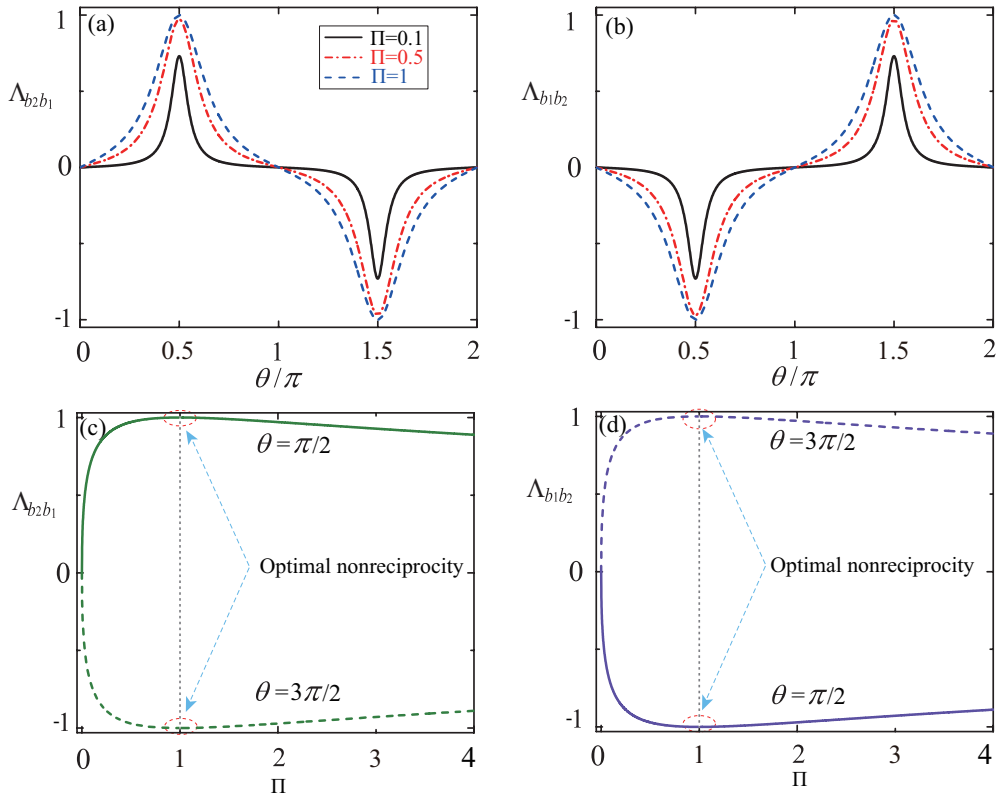

FIG. S7: (Color online) Dependence of the relative phonon-scattering rates (a) $\Lambda_{b_2b_1}$ and (b) $\Lambda_{b_1b_2}$ on the phase θ when $\omega=\omega_m$ and the optomechanical cooperativity takes various values: $\Pi=0.1, 0.5$, and 1. The relative phonon-scattering rates (c) $\Lambda_{b_2b_1}$ and (d) $\Lambda_{b_1b_2}$ versus the ratio of the optomechanical cooperativities Π when $\theta=\pi/2$ and $\theta=3\pi/2$. Here we take $\Delta=\omega_1=\omega_2=\omega_m$, $G_1/\omega_m=G_2/\omega_m=0.1$, $\kappa/\omega_m=0.2$, $\gamma_1/\omega_m=\gamma_2/\omega_m=10^{-5}$, and $\bar{n}_1=\bar{n}_2=10^3$.

the process from b_1 (b_2) to b_2 (b_1) and is zero for the opposite process when $\theta=\pi/2$ ($\theta=3\pi/2$), namely, $T_{b_1b_2}=0$ and $T_{b_2b_1}=0$ at $\theta=\pi/2$ and $\theta=3\pi/2$, respectively.

In order to analyze the optomechanical cooperativities among the two subsystems in this three-mode optomechanical system, we introduce a new parameter defined by $\Pi=\mathcal{C}_3/(\mathcal{C}_1\mathcal{C}_2)$, which is the ratio of the optomechanical cooperativities. Thus, the analytical solutions given in Eqs. (S49a) and (S49b) become

$$\Lambda_{b_2b_1}=\frac{4\sqrt{\Pi}\sin\theta}{(1+\sqrt{\Pi})^2\left[1+\frac{4\Pi\cos^2\theta}{\left(\frac{\mathcal{C}_1+\mathcal{C}_2+1}{\mathcal{C}_1\mathcal{C}_2}+\Pi\right)^2}\right]}, \tag{S50a}$$

$$\Lambda_{b_1b_2}=-\Lambda_{b_2b_1}. \tag{S50b}$$

It can be seen from Eqs. (S50a) and (S50b) that the relative nonreciprocal phonon transfer $\Lambda_{b_2b_1}=1$ ($\Lambda_{b_1b_2}=1$) is obtained at $\Pi=1$ and $\theta=\pi/2$ ($3\pi/2$). In Figs. S7(a) and S7(b), we plot the relative phonon-scattering rates $\Lambda_{b_2b_1}$ and $\Lambda_{b_1b_2}$ as functions of the phase θ when Π takes various values: $\Pi=0.1, 0.5$, and 1. The results show that the optimal nonreciprocity appears at $\Pi=1$ and either $\theta=\pi/2$ or $3\pi/2$. When $\Pi\neq1$, the absolute value of the relative phonon-scattering rate will be decreased at a given phase θ. We also plot the relative phonon-scattering rates $\Lambda_{b_2b_1}$ and $\Lambda_{b_1b_2}$ versus the ratio Π when the phase takes $\theta=\pi/2$ (solid lines) and $\theta=3\pi/2$ (dashed lines), as shown in Figs. S7(c) and S7(d). In the region $0<\Pi<1$, the nonreciprocal phonon-transfer rate $\Lambda_{b_2b_1}$ increases with the increase of Π. In the region $\Pi>1$, the relative nonreciprocal phonon-transfer rate is suppressed. The optimal nonreciprocity emerges at $\Pi=1$, which indicates directional flow of phonons between the two mechanical resonators.

IV. THE COOLING LIMITS OF THE TWO MECHANICAL RESONATORS

In this section, we present a detailed derivation of the cooling limits of the two mechanical resonators, which are obtained by adiabatically eliminating the cavity-field mode in the large cavity-field decay regime. In this case, the system is reduced to a two-coupled mechanical resonator system. The derivation of the cooling limits is based on the Langevin equations (S4) for the quantum fluctuations of the system operators. To obtain the cooling limits, we consider the case where the linearized optomechanical coupling strengths $G_{1,2}$ are real and the system works in the parameter regime:

$$\omega_{1,2} \gg \kappa \gg G_{1,2} \gg \gamma_{1,2}. \tag{S51}$$

In this case, the cavity field can be eliminated adiabatically, and then the solution of the cavity-field fluctuation operator $\delta a(t)$ at the time scale $t \gg 1/\kappa$ can be obtained as

$$\delta a(t) \approx -\frac{iG_1}{\kappa+i(\Delta+\omega_1)}\delta b_1^\dagger(t) - \frac{iG_1}{\kappa+i(\Delta-\omega_1)}\delta b_1(t) - \frac{iG_2}{\kappa+i(\Delta+\omega_2)}\delta b_2^\dagger(t) - \frac{iG_2}{\kappa+i(\Delta-\omega_2)}\delta b_2(t) + F_{a,\mathrm{in}}(t), \tag{S52}$$

where we introduce the new noise operator

$$F_{a,\mathrm{in}}(t) = \sqrt{2\kappa}e^{-(\kappa+i\Delta)t}\int_0^t a_{\mathrm{in}}(s)e^{(\kappa+i\Delta)s}ds. \tag{S53}$$

Substitution of Eq. (S52) into Eqs. (S4b) and (S4c) leads to the equations of motion

$$\begin{aligned}
\delta\dot{b}_1(t) =& \left(\frac{G_1^2}{\kappa-i(\Delta-\omega_1)} - \frac{G_1^2}{\kappa+i(\Delta+\omega_1)}\right)\delta b_1^\dagger(t) + \left(\frac{G_1^2}{\kappa-i(\Delta+\omega_1)} - \frac{G_1^2}{\kappa+i(\Delta-\omega_1)} - (\gamma_1+i\omega_1)\right)\delta b_1(t) \\
&+ \left(\frac{G_1G_2}{\kappa-i(\Delta-\omega_2)} - \frac{G_1G_2}{\kappa+i(\Delta+\omega_2)}\right)\delta b_2^\dagger(t) + \left(\frac{G_1G_2}{\kappa-i(\Delta+\omega_2)} - \frac{G_1G_2}{\kappa+i(\Delta-\omega_2)} - i\eta e^{i\theta}\right)\delta b_2(t) \\
&- iG_1F_{a,\mathrm{in}}(t) - iG_1F_{a,\mathrm{in}}^\dagger(t) + \sqrt{2\gamma_1}b_{1,\mathrm{in}}(t),
\end{aligned} \tag{S54a}$$

$$\begin{aligned}
\delta\dot{b}_2(t) =& \left(\frac{G_1G_2}{\kappa-i(\Delta-\omega_1)} - \frac{G_1G_2}{\kappa+i(\Delta+\omega_1)}\right)\delta b_1^\dagger(t) + \left(\frac{G_1G_2}{\kappa-i(\Delta+\omega_1)} - \frac{G_1G_2}{\kappa+i(\Delta-\omega_1)} - i\eta e^{-i\theta}\right)\delta b_1(t) \\
&+ \left(\frac{G_2^2}{\kappa-i(\Delta-\omega_2)} - \frac{G_2^2}{\kappa+i(\Delta+\omega_2)}\right)\delta b_2^\dagger(t) + \left(-(\gamma_2+i\omega_2) + \frac{G_2^2}{\kappa-i(\Delta+\omega_2)} - \frac{G_2^2}{\kappa+i(\Delta-\omega_2)}\right)\delta b_2(t) \\
&- iG_2F_{a,\mathrm{in}}(t) - iG_2F_{a,\mathrm{in}}^\dagger(t) + \sqrt{2\gamma_2}b_{2,\mathrm{in}}(t).
\end{aligned} \tag{S54b}$$

By making the RWA in Eqs. (S54a) and (S54b), we have

$$\delta\dot{b}_1(t) = -(\Gamma_1+i\Omega_1)\delta b_1(t) + \xi_1\delta b_2(t) - iG_1F_{a,\mathrm{in}}(t) - iG_1F_{a,\mathrm{in}}^\dagger(t) + \sqrt{2\gamma_1}b_{1,\mathrm{in}}(t), \tag{S55a}$$

$$\delta\dot{b}_2(t) = \xi_2\delta b_1(t) - (\Gamma_2+i\Omega_2)\delta b_2(t) - iG_2F_{a,\mathrm{in}}(t) - iG_2F_{a,\mathrm{in}}^\dagger(t) + \sqrt{2\gamma_2}b_{2,\mathrm{in}}(t), \tag{S55b}$$

where we introduce the effective resonance frequency Ω_l and decay rate Γ_l for the lth mechanical resonator

$$\Omega_l = \omega_l - \omega_{l,\mathrm{opt}}, \tag{S56a}$$

$$\Gamma_l = \gamma_l + \gamma_{l,\mathrm{opt}}, \tag{S56b}$$

with

$$\omega_{l,\mathrm{opt}} = \frac{G_l^2(\Delta+\omega_l)}{\kappa^2+(\Delta+\omega_l)^2} + \frac{G_l^2(\Delta-\omega_l)}{\kappa^2+(\Delta-\omega_l)^2}, \tag{S57a}$$

$$\gamma_{l,\mathrm{opt}} = \frac{G_l^2\kappa}{\kappa^2+(\Delta-\omega_l)^2} - \frac{G_l^2\kappa}{\kappa^2+(\Delta+\omega_l)^2}, \qquad l=1,2. \tag{S57b}$$

Here, $\omega_{l,\mathrm{opt}}$ and $\gamma_{l,\mathrm{opt}}$ denote the resonance frequency shift and the additional energy decay rate induced by the optomechanical couplings, respectively. We also introduce the effective coupling strengths between the two mechanical

modes b_1 and b_2 after adiabatically eliminating the cavity mode as

$$\xi_1 = \frac{G_1G_2[\kappa + i(\Delta+\omega_2)]}{\kappa^2+(\Delta+\omega_2)^2} - \frac{G_1G_2[\kappa - i(\Delta-\omega_2)]}{\kappa^2+(\Delta-\omega_2)^2} - i\eta e^{i\theta}, \tag{S58a}$$

$$\xi_2 = \frac{G_1G_2[\kappa + i(\Delta+\omega_1)]}{\kappa^2+(\Delta+\omega_1)^2} - \frac{G_1G_2[\kappa - i(\Delta-\omega_1)]}{\kappa^2+(\Delta-\omega_1)^2} - i\eta e^{-i\theta}. \tag{S58b}$$

Under the parameter condition $\omega_{1,2} \gg \kappa \gg G_{1,2}$ and at resonance $\Delta = \omega_1 = \omega_2$, we have

$$\xi_1 \approx -\left[\frac{G_1G_2}{\kappa} + i\left(\eta e^{i\theta} - \frac{G_1G_2}{2\omega_2}\right)\right], \tag{S59a}$$

$$\xi_2 \approx -\left[\frac{G_1G_2}{\kappa} + i\left(\eta e^{-i\theta} - \frac{G_1G_2}{2\omega_1}\right)\right], \tag{S59b}$$

and

$$\gamma_{l,\mathrm{opt}} \approx \frac{G_l^2}{\kappa}, \tag{S60a}$$

$$\omega_{l,\mathrm{opt}} \approx \frac{G_l^2}{2\omega_l}, \qquad l = 1, 2. \tag{S60b}$$

The final average phonon numbers (namely the steady-state values of the phonon numbers) can be obtained by solving Eq. (S55). To be concise, we reexpress Eq. (S55) as

$$\dot{\mathbf{v}}(t) = -\mathbf{M}\mathbf{v}(t) + \mathbf{N}(t), \tag{S61}$$

where $\mathbf{v}(t) = (\delta b_1(t), \delta b_2(t))^T$, $\mathbf{M}$ is defined by

$$\mathbf{M} = \begin{pmatrix} \Gamma_1 + i\Omega_1 & -\xi_1 \\ -\xi_2 & \Gamma_2 + i\Omega_2 \end{pmatrix}, \tag{S62}$$

and $\mathbf{N}(t)$ reads

$$\mathbf{N}(t) = \begin{pmatrix} -iG_1F_{a,\mathrm{in}}(t) - iG_1F_{a,\mathrm{in}}^\dagger(t) + \sqrt{2\gamma_1}b_{\mathrm{in},1}(t) \\ -iG_2F_{a,\mathrm{in}}(t) - iG_2F_{a,\mathrm{in}}^\dagger(t) + \sqrt{2\gamma_2}b_{\mathrm{in},2}(t) \end{pmatrix}. \tag{S63}$$

The formal solution of Eq. (S61) can be expressed as

$$\mathbf{v}(t) = e^{-\mathbf{M}t}\mathbf{v}(0) + e^{-\mathbf{M}t}\int_0^t e^{\mathbf{M}\mathbf{s}}\mathbf{N}(s)ds. \tag{S64}$$

The final average phonon numbers can be obtained by calculating the elements of the variance matrix. By a lengthy calculation, we obtain the approximate analytical expressions for the final average phonon numbers as

$$\begin{aligned} n_1^f \;=\; & \frac{\gamma_1\bar{n}_1}{2|u|^2}\Bigg[\frac{|[u-\Gamma_1+\Gamma_2-i(\Omega_1-\Omega_2)]|^2}{\lambda_1^*+\lambda_1} + 2\mathrm{Re}\Big[\frac{[u^*-\Gamma_1+\Gamma_2+i(\Omega_1-\Omega_2)][u+\Gamma_1-\Gamma_2+i(\Omega_1-\Omega_2)]}{\lambda_1^*+\lambda_2}\Big] \\ & + \frac{|[u+\Gamma_1-\Gamma_2+i(\Omega_1-\Omega_2)]|^2}{\lambda_2^*+\lambda_2}\Bigg] + \frac{G_1^2}{4|u|^2}\Bigg[\frac{|[u-\Gamma_1+\Gamma_2-i(\Omega_1-\Omega_2)]|^2}{\lambda_1^*+\lambda_1}\Big(\frac{1}{\kappa+\lambda_1+i\Delta}+\frac{1}{\kappa+\lambda_1^*-i\Delta}\Big) \\ & + 2\mathrm{Re}\Big[\frac{[u^*-\Gamma_1+\Gamma_2+i(\Omega_1-\Omega_2)][u+\Gamma_1-\Gamma_2+i(\Omega_1-\Omega_2)]}{\lambda_1^*+\lambda_2}\Big(\frac{1}{\kappa+\lambda_2+i\Delta}+\frac{1}{\kappa+\lambda_1^*-i\Delta}\Big)\Big] \\ & + \frac{|[u+\Gamma_1-\Gamma_2+i(\Omega_1-\Omega_2)]|^2}{\lambda_2^*+\lambda_2}\Big(\frac{1}{\kappa+\lambda_2+i\Delta}+\frac{1}{\kappa+\lambda_2^*-i\Delta}\Big)\Bigg] \\ & + \frac{|\xi_1|^2}{|u|^2}\Bigg[G_2^2\Bigg[\frac{1}{\lambda_1^*+\lambda_1}\Big(\frac{1}{\kappa+\lambda_1+i\Delta}+\frac{1}{\kappa+\lambda_1^*-i\Delta}\Big) - 2\mathrm{Re}\Big[\frac{1}{\lambda_1^*+\lambda_2}\Big(\frac{1}{\kappa+\lambda_2+i\Delta}+\frac{1}{\kappa+\lambda_1^*-i\Delta}\Big)\Big] \\ & + \frac{1}{\lambda_2^*+\lambda_2}\Big(\frac{1}{\kappa+\lambda_2+i\Delta}+\frac{1}{\kappa+\lambda_2^*-i\Delta}\Big)\Bigg] + 2\gamma_2\bar{n}_2\Big(\frac{1}{\lambda_1^*+\lambda_1} - \frac{1}{\lambda_1^*+\lambda_2} - \frac{1}{\lambda_2^*+\lambda_1} + \frac{1}{\lambda_2^*+\lambda_2}\Big)\Bigg], \end{aligned} \tag{S65}$$

and

$$
\begin{aligned}
n_2^f \;=\; & \frac{\gamma_2\bar{n}_2}{2|u|^2}\Bigg[\frac{|u+\Gamma_1-\Gamma_2+i(\Omega_1-\Omega_2)|^2}{\lambda_1^*+\lambda_1}+2\mathrm{Re}\Big[\frac{[u^*+\Gamma_1-\Gamma_2-i(\Omega_1-\Omega_2)][u-\Gamma_1+\Gamma_2-i(\Omega_1-\Omega_2)]}{\lambda_1^*+\lambda_2}\Big] \\
& +\frac{|u-\Gamma_1+\Gamma_2-i(\Omega_1-\Omega_2)|^2}{\lambda_2^*+\lambda_2}\Bigg]+\frac{G_2^2}{4|u|^2}\Bigg[\frac{|u+\Gamma_1-\Gamma_2+i(\Omega_1-\Omega_2)|^2}{\lambda_1^*+\lambda_1}\Big(\frac{1}{\kappa+\lambda_1+i\Delta}+\frac{1}{\kappa+\lambda_1^*-i\Delta}\Big) \\
& +2\mathrm{Re}\Big[\frac{[u-\Gamma_1+\Gamma_2-i(\Omega_1-\Omega_2)][u^*+\Gamma_1-\Gamma_2-i(\Omega_1-\Omega_2)]}{\lambda_1^*+\lambda_2}\Big(\frac{1}{\kappa+\lambda_2+i\Delta}+\frac{1}{\kappa+\lambda_1^*-i\Delta}\Big)\Big] \\
& +\frac{|u-\Gamma_1+\Gamma_2-i(\Omega_1-\Omega_2)|^2}{\lambda_2^*+\lambda_2}\Big(\frac{1}{\kappa+\lambda_2+i\Delta}+\frac{1}{\kappa+\lambda_2^*-i\Delta}\Big)\Bigg] \\
& +\frac{|\xi_2|^2}{|u|^2}\Bigg[G_1^2\Bigg[\frac{1}{\lambda_1^*+\lambda_1}\Big(\frac{1}{\kappa+\lambda_1+i\Delta}+\frac{1}{\kappa+\lambda_1^*-i\Delta}\Big)-2\mathrm{Re}\Big[\frac{1}{\lambda_2+\lambda_1^*}\Big(\frac{1}{\kappa+\lambda_2+i\Delta}+\frac{1}{\kappa+\lambda_1^*-i\Delta}\Big)\Big] \\
& +\frac{1}{\lambda_2^*+\lambda_2}\Big(\frac{1}{\kappa+\lambda_2+i\Delta}+\frac{1}{\kappa+\lambda_2^*-i\Delta}\Big)\Bigg]+2\gamma_1\bar{n}_1\Big(\frac{1}{\lambda_1^*+\lambda_1}-\frac{1}{\lambda_1^*+\lambda_2}-\frac{1}{\lambda_2^*+\lambda_1}+\frac{1}{\lambda_2^*+\lambda_2}\Big)\Bigg],
\end{aligned}
\tag{S66}
$$

where λ_1 and λ_2 (λ_1^* and λ_2^* being complex conjugate) are the eigenvalues of the coefficient matrix $\mathbf{M}$,

$$
\lambda_1 = \frac{1}{2}[\Gamma_1+\Gamma_2+i(\Omega_1+\Omega_2)-u], \tag{S67a}
$$

$$
\lambda_2 = \frac{1}{2}[\Gamma_1+\Gamma_2+i(\Omega_1+\Omega_2)+u] \tag{S67b}
$$

where

$$
u=\sqrt{4\xi_1\xi_2+[\Gamma_1-\Gamma_2+i(\Omega_1-\Omega_2)]^2}. \tag{S68}
$$

For the case $\omega_1 \approx \omega_2$ and $\Gamma_1 \approx \Gamma_2$, the approximate analytical expressions of the final average phonon numbers can be reduced as

$$
\begin{aligned}
n_1^f \;\approx\; & \frac{\gamma_1\bar{n}_1}{2}\Big(\frac{1}{\lambda_1^*+\lambda_1}+2\mathrm{Re}\Big[\frac{1}{\lambda_1^*+\lambda_2}\Big]+\frac{1}{\lambda_2^*+\lambda_2}\Big)+\frac{G_1^2}{4}\Bigg[\frac{1}{\lambda_1^*+\lambda_1}\Big(\frac{1}{\kappa+\lambda_1+i\Delta}+\frac{1}{\kappa+\lambda_1^*-i\Delta}\Big) \\
& +2\mathrm{Re}\Big[\frac{1}{\lambda_1^*+\lambda_2}\Big(\frac{1}{\kappa+\lambda_2+i\Delta}+\frac{1}{\kappa+\lambda_1^*-i\Delta}\Big)\Big]+\frac{1}{\lambda_2^*+\lambda_2}\Big(\frac{1}{\kappa+\lambda_2+i\Delta}+\frac{1}{\kappa+\lambda_2^*-i\Delta}\Big)\Bigg] \\
& +\frac{|\xi_1|}{4|\xi_2|}\Bigg[G_2^2\Bigg[\frac{1}{\lambda_1^*+\lambda_1}\Big(\frac{1}{\kappa+\lambda_1+i\Delta}+\frac{1}{\kappa+\lambda_1^*-i\Delta}\Big)-2\mathrm{Re}\Big[\frac{1}{\lambda_1^*+\lambda_2}\Big(\frac{1}{\kappa+\lambda_2+i\Delta}+\frac{1}{\kappa+\lambda_1^*-i\Delta}\Big)\Big] \\
& +\frac{1}{\lambda_2^*+\lambda_2}\Big(\frac{1}{\kappa+\lambda_2+i\Delta}+\frac{1}{\kappa+\lambda_2^*-i\Delta}\Big)\Bigg]+2\gamma_2\bar{n}_2\Big(\frac{1}{\lambda_1^*+\lambda_1}-2\mathrm{Re}\Big[\frac{1}{\lambda_1^*+\lambda_2}\Big]+\frac{1}{\lambda_2^*+\lambda_2}\Big)\Bigg],
\end{aligned}
\tag{S69}
$$

and

$$
\begin{aligned}
n_2^f \;\approx\; & \frac{\gamma_2\bar{n}_2}{2}\Big(\frac{1}{\lambda_1^*+\lambda_1}+2\mathrm{Re}\Big[\frac{1}{\lambda_1^*+\lambda_2}\Big]+\frac{1}{\lambda_2^*+\lambda_2}\Big)+\frac{G_2^2}{4}\Bigg[\frac{1}{\lambda_1^*+\lambda_1}\Big(\frac{1}{\kappa+\lambda_1+i\Delta}+\frac{1}{\kappa+\lambda_1^*-i\Delta}\Big) \\
& +2\mathrm{Re}\Big[\frac{1}{\lambda_1^*+\lambda_2}\Big(\frac{1}{\kappa+\lambda_2+i\Delta}+\frac{1}{\kappa+\lambda_1^*-i\Delta}\Big)\Big]+\frac{1}{\lambda_2^*+\lambda_2}\Big(\frac{1}{\kappa+\lambda_2+i\Delta}+\frac{1}{\kappa+\lambda_2^*-i\Delta}\Big)\Bigg] \\
& +\frac{|\xi_2|}{4|\xi_1|}\Bigg[G_1^2\Bigg[\frac{1}{\lambda_1^*+\lambda_1}\Big(\frac{1}{\kappa+\lambda_1+i\Delta}+\frac{1}{\kappa+\lambda_1^*-i\Delta}\Big)-2\mathrm{Re}\Big[\frac{1}{\lambda_1^*+\lambda_2}\Big(\frac{1}{\kappa+\lambda_2+i\Delta}+\frac{1}{\kappa+\lambda_1^*-i\Delta}\Big)\Big] \\
& +\frac{1}{\lambda_2^*+\lambda_2}\Big(\frac{1}{\kappa+\lambda_2+i\Delta}+\frac{1}{\kappa+\lambda_2^*-i\Delta}\Big)\Bigg]+2\gamma_1\bar{n}_1\Big(\frac{1}{\lambda_1^*+\lambda_1}-2\mathrm{Re}\Big[\frac{1}{\lambda_1^*+\lambda_2}\Big]+\frac{1}{\lambda_2^*+\lambda_2}\Big)\Bigg].
\end{aligned}
\tag{S70}
$$

By substituting Eq. (S67) into Eqs. (S69) and (S70) and considering the parameters relations $\omega_{1,2} \gg \kappa \gg G_{1,2} \gg \{\gamma_{1,\mathrm{opt}} \approx \gamma_{2,\mathrm{opt}}\} \gg \gamma_{1,2}$, the final average phonon numbers can be simplified as

$$
n_{l=1,2}^f \;\approx\; \frac{\gamma_l\bar{n}_l+\gamma_{l,\mathrm{opt}}n_{\mathrm{opt}}}{\Gamma_l+\chi_+}+\frac{(-1)^{l-1}\sqrt{\chi_l}(\sqrt{\chi_1}n_{\chi_1}-\sqrt{\chi_2}n_{\chi_2})}{\Gamma_l+\chi_-}, \tag{S71}
$$

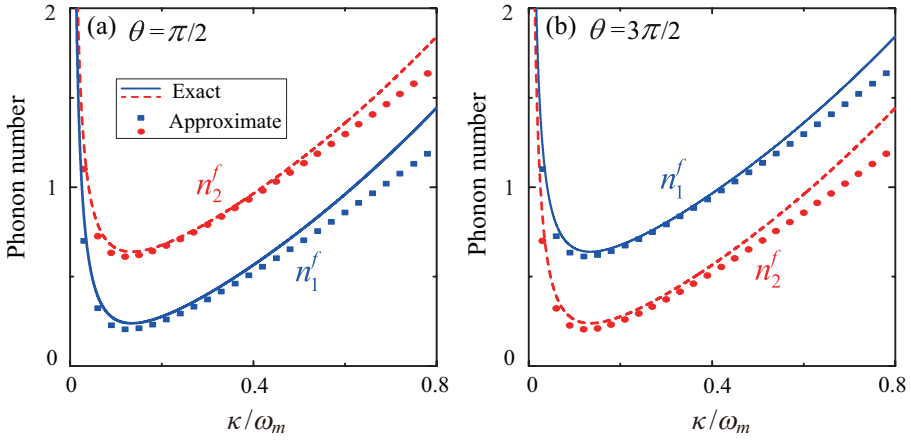

FIG. S8: (Color online) The final average phonon numbers n_1^f and n_2^f are plotted as functions of κ/ω_m when the phase θ takes the values: (a) $\theta=\pi/2$ and (b) $\theta=3\pi/2$. The exact results are given by Eq. (S28) (solid curves) and the approximate results obtained by the adiabatic elimination method are given by Eq. (S71) (symbols). Here, the used parameters are $\Delta=\omega_1=\omega_2=\omega_m$, $G_1/\omega_m=G_2/\omega_m=0.08$, $\eta/\omega_m=0.05$, $\gamma_1/\omega_m=\gamma_2/\omega_m=10^{-5}$, and $\bar{n}_1=\bar{n}_2=1000$.

where we introduce the following variables

$$n_{\rm opt}=\frac{4\kappa^2}{(\omega_1+\omega_2+2\Delta)^2}, \tag{S72a}$$

$$n_{\chi_{1(2)}}=\frac{2(\gamma_{2(1)}\bar{n}_{2(1)}+\gamma_{2(1)\rm opt}n_{\rm opt})}{\Gamma_1+\Gamma_2+2\chi_+}, \tag{S72b}$$

$$\chi_\pm=\mp\sqrt{\chi_1\chi_2}-{\rm Re}\left[\frac{\xi_1\xi_2}{\Gamma_1+\Gamma_2}\right], \tag{S72c}$$

$$\chi_{l=1,2}=\frac{|\xi_l|^2}{\Gamma_1+\Gamma_2}. \tag{S72d}$$

Here, $n_{\rm opt}$ stands for the effective phonon number in the optomechanical cooling bath, and χ_1 and χ_2 are the effective phonon-transfer rates from b_2 to b_1 and from b_1 to b_2, respectively. The corresponding cooling limits ($n_1^{\rm lim}$, $n_2^{\rm lim}$) are obtained by taking the optimal driving detuning $\Delta=\omega_l$ in Eq. (S71). In particular, the first term in Eq. (S71) is contributed by the thermal bath and the effective optical bath connected by the lth mechanical resonator, while the phonon extraction contribution induced by the phonon-exchange channel is presented by the last term. Physically, the nonreciprocity of the phonon transfer is decided by the phonon-exchange rate χ_l which depends on the phase θ. In the case $\bar{n}_1\approx\bar{n}_2$ and $\gamma_1\approx\gamma_2$, we have $n_{\chi_1}\approx n_{\chi_2}=n_\chi$ and thus $(\sqrt{\chi_1}n_{\chi_1}-\sqrt{\chi_2}n_{\chi_2})\approx(\sqrt{\chi_1}-\sqrt{\chi_2})n_\chi$. In the region $0<\theta<\pi$ ($\pi<\theta<2\pi$), we obtain $\sqrt{\chi_1}<\sqrt{\chi_2}$ ($\sqrt{\chi_1}>\sqrt{\chi_2}$). This means that the phonon-transfer rate from b_1 (b_2) to b_2 (b_1) is larger than that for the opposite case. According to Eq. (S71), we then have the relation $n_1^f<n_2^f$ ($n_1^f>n_2^f$) in the region $0<\theta<\pi$ ($\pi<\theta<2\pi$). When $\theta=\pi/2$ ($3\pi/2$) and $\sqrt{\mathcal{C}_1\mathcal{C}_2}=\sqrt{\mathcal{C}_3}$, the unidirectional flow of the phonons between the two mechanical resonators is achieved [$\chi_1\approx0$ ($\chi_2\approx0$)]. For $\theta=n\pi$, the phonon transfer between the two mechanical resonators is reciprocal ($\sqrt{\chi_1}=\sqrt{\chi_2}$), due to the emergence of the dark mode. Once the phonon-transfer channel is turned off ($\eta=0$), the ground-state cooling is unfeasible owing to the invalid effective cooling channel ($\Gamma_l+\chi_+\to\gamma_l$). In the absence of the optomechanical cooling channels ($G_{1,2}=0$), Eq. (S71) becomes $n_{l=1,2}^f\approx\bar{n}_l+(-1)^{l-1}(n_{\chi_1}-n_{\chi_2})/2$, which indicates quantum thermalization in this coupled mechanical system.

Moreover, both the exact and approximate final average phonon numbers n_1^f and n_2^f are plotted in Fig. S8 as functions of the cavity-field decay rate κ at the optimal driving detuning $\Delta=\omega_m$ when the modulation phase θ takes various values: (a) $\theta=\pi/2$ and (b) $\theta=3\pi/2$. Here, the blue solid curves (n_1^f) and the red dashed curves (n_2^f) are plotted using the exact solutions given in Eq. (S28), while the symbols are based on the analytical calculations given in Eq. (S71). We can see from Fig. S8 that the analytical cooling limits and the exact results match well with each other when $\kappa/\omega_m<0.4$, and the difference between the numerical simulation and approximate results increases when $\kappa/\omega_m>0.4$. This means that the cooling performances of the two mechanical resonators are excellent in the resolved-sideband regime ($\kappa\ll\omega_m$). This result is consistent with the sideband cooling results in the typical optomechanical systems. We also see from Fig. S8(a) that the cooling performance of the first resonator is better than that of the second resonator ($n_1^f<n_2^f$) when $\theta=\pi/2$. However, when $\theta=3\pi/2$, the opposite cooling performance ($n_1^f>n_2^f$)

has been displayed in comparison with the case of $\theta = \pi/2$, as shown in Fig. S8(b). Physically, the nonreciprocal phonon-transfer mechanism is more helpful to cool the first (second) resonator when $0 < \theta < \pi$ ($\pi < \theta < 2\pi$). In particular, the optimal cooling performances of the two mechanical resonators require that the working value of cavity-field decay rate is around $\kappa/\omega_m = 0.1 \sim 0.2$, as shown in Fig. S8. This is a result of the competition between the efficiency of extraction of the thermal excitations and the phonon-sideband resolution condition. When $\kappa/\omega_m < 0.1$, the cooling performances of the two mechanical resonators become worse. Physically, the vacuum bath of the cavity field extracts the thermal excitations in the two mechanical resonators through a manner of nonequilibrium dynamics, and then the total system reaches a steady state. When the cavity-field decay rate κ is equal to 0, the vacuum bath cannot extract the thermal phonons in these two mechanical resonators, and then this system will be thermalized to a thermal equilibrium state.

V. THE DARK-MODE EFFECT AND ITS BREAKING IN A MULTIPLE-MECHANICAL-RESONATOR OPTOMECHANICAL SYSTEM

In this section, we study the dark-mode effect in a multiple-mechanical-resonator optomechanical system, which consists of one cavity mode and N ($N \geq 3$) mechanical resonators [see Figs. S9(a) and S9(b)]. The Hamiltonian of this system can be written in a frame rotating at the driving frequency ω_L as

$$H_I = \Delta_c a^\dagger a + \sum_{j=1}^{N} \omega_j b_j^\dagger b_j + \sum_{j=1}^{N} g_j a^\dagger a (b_j + b_j^\dagger) + (\Omega a + \Omega^* a^\dagger) + \sum_{j=1}^{N-1} \eta_j (e^{i\theta_j} b_j^\dagger b_{j+1} + \text{H.c.}), \tag{S73}$$

where $\Delta_c = \omega_c - \omega_L$ is the detuning of the cavity-field resonance frequency ω_c with respect to the driving frequency ω_L. The operators a ($a^\dagger$) and b_j ($b_j^\dagger$) are, respectively, the annihilation (creation) operators of the cavity-field mode and the jth mechanical resonator (with the resonance frequency ω_j). The optomechanical interactions between the cavity mode and the jth mechanical resonator are described by the g_j terms (with g_j being the single-photon optomechanical-coupling strength). The cavity-field driving is denoted by the Ω term (with Ω being the driving amplitude). To manipulate the energy exchange between the neighboring mechanical resonators, we introduce a phase-dependent phonon-exchange interaction between the neighboring mechanical resonators, with the coupling strength η_j and the phase θ_j. By phenomenologically adding the damping and noise terms into the Heisenberg equations obtained based on the Hamiltonian in Eq. (S73), the quantum Langevin equations for the operators of the optical and mechanical modes can be obtained as

$$\begin{aligned}
\dot{a} &= -ia[\Delta_c + g_1(b_1 + b_1^\dagger) + g_2(b_2 + b_2^\dagger) + \cdots + g_N(b_N + b_N^\dagger)] - i\Omega - \kappa a + \sqrt{2\kappa} a_{\text{in}}, \\
\dot{b}_1 &= -(\gamma_1 + i\omega_1) b_1 - i g_1 a^\dagger a - i\eta_1 e^{i\theta_1} b_2 + \sqrt{2\gamma_1} b_{1,\text{in}}, \\
\dot{b}_2 &= -(\gamma_2 + i\omega_2) b_2 - i g_2 a^\dagger a - i\eta_1 e^{-i\theta_1} b_1 - i\eta_2 e^{i\theta_2} b_3 + \sqrt{2\gamma_2} b_{2,\text{in}}, \\
\dot{b}_3 &= -(\gamma_3 + i\omega_3) b_3 - i g_3 a^\dagger a - i\eta_2 e^{-i\theta_2} b_2 - i\eta_3 e^{i\theta_3} b_4 + \sqrt{2\gamma_3} b_{3,\text{in}}, \\
\dot{b}_4 &= -(\gamma_4 + i\omega_4) b_4 - i g_4 a^\dagger a - i\eta_3 e^{-i\theta_3} b_3 - i\eta_4 e^{i\theta_4} b_5 + \sqrt{2\gamma_4} b_{4,\text{in}}, \\
&\vdots \\
\dot{b}_{N-1} &= -(\gamma_{N-1} + i\omega_{N-1}) b_{N-1} - i g_{N-1} a^\dagger a - i\eta_{N-2} e^{-i\theta_{N-2}} b_{N-2} - i\eta_{N-1} e^{i\theta_{N-1}} b_N + \sqrt{2\gamma_{N-1}} b_{N-1,\text{in}}, \\
\dot{b}_N &= -(\gamma_N + i\omega_N) b_N - i g_N a^\dagger a - i\eta_{N-1} e^{-i\theta_{N-1}} b_{N-1} + \sqrt{2\gamma_N} b_{N,\text{in}}.
\end{aligned} \tag{S74}$$

To cool the mechanical resonators, we consider the strong-driving regime of the cavity field such that the average photon number in the cavity is sufficiently large and then the linearization procedure can be used to simplify the physical model. To this end, we express the operators in Eq. (S74) as the sum of their steady-state mean values and quantum fluctuations, namely $o = \langle o \rangle_{\text{ss}} + \delta o$ for operators a, $a^\dagger$, $b_{j=1-N}$, and $b_j^\dagger$. By separating the classical motion

and the quantum fluctuation, the linearized equations of motion for the quantum fluctuations can be written as

$$\begin{aligned}
\frac{d}{dt}\delta a &= -(\kappa+i\Delta)\delta a - i\alpha[g_1(\delta b_1+\delta b_1^\dagger)+g_2(\delta b_2+\delta b_2^\dagger)+\cdots+g_{N-1}(\delta b_{N-1}+\delta b_{N-1}^\dagger)\\
&\quad +g_N(\delta b_N+\delta b_N^\dagger)]+\sqrt{2\kappa}a_{\rm in},\\
\frac{d}{dt}\delta b_1 &= -(\gamma_1+i\omega_1)\delta b_1 - ig_1\alpha^*\delta a - ig_1\alpha\delta a^\dagger - i\eta_1 e^{i\theta_1}\delta b_2+\sqrt{2\gamma_1}b_{1,\rm in},\\
\frac{d}{dt}\delta b_2 &= -(\gamma_2+i\omega_2)\delta b_2 - ig_2\alpha^*\delta a - ig_2\alpha\delta a^\dagger - i\eta_1 e^{-i\theta_1}\delta b_1 - i\eta_2 e^{i\theta_2}\delta b_3+\sqrt{2\gamma_2}b_{2,\rm in},\\
\frac{d}{dt}\delta b_3 &= -(\gamma_3+i\omega_3)\delta b_3 - ig_3\alpha^*\delta a - ig_3\alpha\delta a^\dagger - i\eta_2 e^{-i\theta_2}\delta b_2 - i\eta_3 e^{i\theta_3}\delta b_4+\sqrt{2\gamma_3}b_{3,\rm in},\\
\frac{d}{dt}\delta b_4 &= -(\gamma_4+i\omega_4)\delta b_4 - ig_4\alpha^*\delta a - ig_4\alpha\delta a^\dagger - i\eta_3 e^{-i\theta_3}\delta b_3 - i\eta_4 e^{i\theta_4}\delta b_5+\sqrt{2\gamma_4}b_{4,\rm in}\\
&\vdots\\
\frac{d}{dt}\delta b_{N-1} &= -(\gamma_{N-1}+i\omega_{N-1})\delta b_{N-1} - ig_{N-1}\alpha^*\delta a - ig_{N-1}\alpha\delta a^\dagger - i\eta_{N-2}e^{-i\theta_{N-2}}\delta b_{N-2}\\
&\quad -i\eta_{N-1}e^{i\theta_{N-1}}\delta b_N+\sqrt{2\gamma_{N-1}}b_{N-1,\rm in},\\
\frac{d}{dt}\delta b_N &= -(\gamma_N+i\omega_N)\delta b_N - ig_N\alpha^*\delta a - ig_N\alpha\delta a^\dagger - i\eta_{N-1}e^{-i\theta_{N-1}}\delta b_{N-1}+\sqrt{2\gamma_N}b_{N,\rm in}.
\end{aligned}\tag{S75}$$

Based on Eqs. (S75), we adopt the same procedure as that used in the two-mechanical-resonator case to infer a linearized optomechanical Hamiltonian governing the evolution of quantum fluctuations. For studying quantum cooling of these mechanical resonators, we focus on the beam-splitting-type interactions (i.e., the rotating-wave interaction term) between these bosonic modes because these terms dominate the linearized couplings in this system, and hence we can simplify the Hamiltonian of the system by making the RWA. The linearized optomechanical Hamiltonian under the RWA is given by

$$H_I = \Delta\delta a^\dagger\delta a+\omega_j\textstyle\sum_{j=1}^N\delta b_j^\dagger\delta b_j+\sum_{j=1}^N G_j(\delta a^\dagger\delta b_j+\delta b_j^\dagger\delta a)+H_{\rm mrc},\tag{S76}$$

where $\Delta=\Delta_c+\sum_{j=1}^N g_j(\beta_j+\beta_j^*)$ is the normalized driving detuning after the linearization, and $G_j=g_j|\alpha|$ is the linearized optomechanical coupling strength between the jth mechanical resonator and the cavity-field mode. The interaction Hamiltonians between the neighboring mechanical resonators are given by

$$H_{\rm mrc} = \textstyle\sum_{j=1}^{N-1}H_j,\tag{S77}$$

with

$$H_j = \eta_j(e^{-i\theta_j}\delta b_j\delta b_{j+1}^\dagger+e^{i\theta_j}\delta b_{j+1}\delta b_j^\dagger),\tag{S78}$$

which describes the phonon-exchange interaction between the jth resonator and the $(j+1)$th resonator.

In order to investigate the dark-mode effect in the N-mechanical-resonator optomechanical system, we firstly consider the case where the phonon-exchange interaction between the neighbouring mechanical resonators is absent, i.e., $H_{\rm mrc}=0$, as shown in Fig. S9(a). For convenience, we assume that all the mechanical resonators have the same resonance frequencies ($\omega_j=\omega_m$) and optomechanical coupling strengths ($G_j=G$). In this system, there exists a bright mode $B_+=\sum_{j=1}^N\delta b_j/\sqrt{N}$ and $(N-1)$ dark modes which decouple from the cavity-field mode. As a result, the phonons stored in these dark modes cannot be extracted though the optomechanical cooling channel, and then these mechanical resonators cannot be cooled to their quantum ground states. Here, we can obtain the cooling limits of the N mechanical resonators, which are given by $\bar{n}(N-1)/N$. The result shows that in the presence of the dark-mode effect, the final average phonon numbers in these mechanical resonators depend on the number of the mechanical resonators. In this case, the ground-state cooling cannot be realized in these mechanical resonators. In particular, the final average phonon numbers in these mechanical resonators are approximately equal to the thermal excitations in their heat baths when $N\gg 1$ and hence $\bar{n}(N-1)/N\approx\bar{n}$.

To break the dark-mode effect and realize the simultaneous ground-state cooling in the N-mechanical-resonator optomechanical system, the phase-dependent phonon-exchange interaction $H_{\rm mrc}$ should be introduced, as shown in Fig. S9(b). Without loss of generality, we assume that all the coupling strengths of the phonon-exchange interactions are same $\eta_j=\eta$. Thus, we can diagonalize the Hamiltonian of these coupled mechanical resonators as

$$H_{\rm mrt} = \omega_m\sum_{j=1}^N\delta b_j^\dagger\delta b_j+\eta\sum_{j=1}^{N-1}(e^{-i\theta_j}\delta b_j\delta b_{j+1}^\dagger+e^{i\theta_j}\delta b_{j+1}\delta b_j^\dagger)=\sum_{k=1}^N\Omega_k B_k^\dagger B_k,\tag{S79}$$

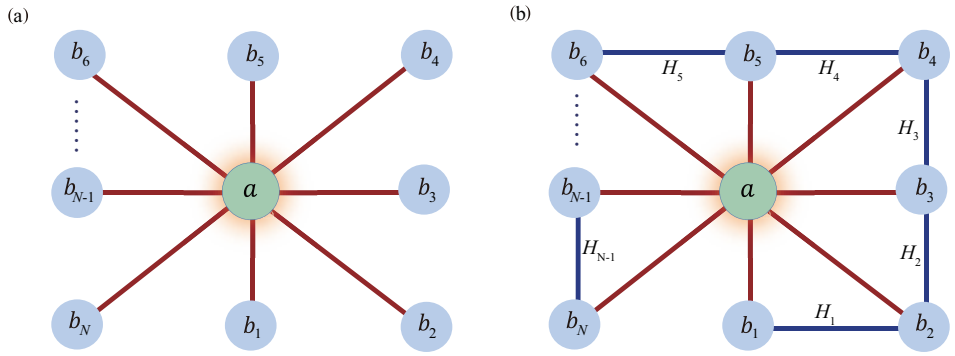

FIG. S9: (Color online) (a) The N-mechanical-resonator optomechanical system: a cavity-field mode simultaneously couples to N mechanical resonators through the optomechanical interactions. (b) The phonon-exchange interactions between two neighboring mechanical resonators are introduced into the N-mechanical-resonator optomechanical system described by panel (a). Note that there is no direct coupling between the first resonator and the Nth resonator.

where B_k is the kth mechanical normal mode with the resonance frequency Ω_k given by

$$\Omega_k = \omega_m + 2\eta \cos\left(\frac{k\pi}{N+1}\right), \qquad k = 1, 2, 3, ..., N. \tag{S80}$$

The relationship between the mechanical modes δb_j and the normal modes B_k is given by

$$\delta b_j = \begin{cases} \frac{1}{A}\sum_{k=1}^{N} \sin\left(\frac{k\pi}{N+1}\right) B_k, & j = 1, \\ \frac{1}{A} e^{-i\sum_{\nu=1}^{j-1}\theta_\nu} \sum_{k=1}^{N} \sin\left(\frac{jk\pi}{N+1}\right) B_k, & j \geq 2, \end{cases} \tag{S81}$$

where we introduce the variable

$$A = \sqrt{\frac{N+1}{2}}. \tag{S82}$$

The Hamiltonian in Eq. (S76) can be rewritten with these mechanical normal modes as

$$H_I = \Delta \delta a^\dagger \delta a + \sum_{k=1}^{N} \Omega_k B_k^\dagger B_k + H_{\rm om}, \tag{S83}$$

where the optomechanical Hamiltonian $H_{\rm om}$ reads

$$H_{\rm om} = \frac{G}{A}\sum_{k=1}^{N}\left[\sin\left(\frac{k\pi}{N+1}\right) + \sum_{j=2}^{N} e^{i\sum_{\nu=1}^{j-1}\theta_\nu} \sin\left(\frac{jk\pi}{N+1}\right)\right] a B_k^\dagger + \text{H.c.}. \tag{S84}$$

It can be seen from Eq. (S84) that the function of these phases in the optomechanical interactions is determined by the term $\sum_{\nu=1}^{j-1}\theta_\nu$. Hence, we can apply a single phase to realize the dark-mode-breaking task. For simplicity, we assume $\theta_j = 0$ for $j = 2$-$(N-1)$ in the following discussions.

As a special case, we first analyze the case of $N = 2$. In this case, the multiple-mechanical-resonator optomechanical system is reduced to the two-mechanical-resonator optomechanical system, which has been analyzed before. When $N = 2$, the optomechanical interaction reads

$$H_{\rm om} = \frac{\sqrt{2}G}{2}(1 + e^{i\theta_1}) a B_1^\dagger + \frac{\sqrt{2}G}{2}(1 - e^{i\theta_1}) a B_2^\dagger + \text{H.c.}. \tag{S85}$$

It is obvious that when $\theta = n\pi$ for an integer n, the cavity field is decoupled from one of the two hybrid mechanical modes: either B_1 or B_2. This hybrid mechanical mode decoupled from the cavity mode is the dark mode. However, in a general case $\theta \neq n\pi$, the dark-mode effect is broken, and then the ground-state cooling becomes accessible under proper parameter conditions.

For the case of $N \geq 3$, the effective coupling coefficient between the cavity-field mode a and the kth normal mode B_k in Eq. (S84) can be expressed as

$$\begin{aligned}
&\frac{G}{A}\left[\sin\left(\frac{k\pi}{N+1}\right)+\sum_{j=2}^{N} e^{i\sum_{\nu=1}^{j-1}\theta_\nu}\sin\left(\frac{jk\pi}{N+1}\right)\right] \\
=\;& \frac{G}{A}\Bigg[\sin\left(\frac{k\pi}{N+1}\right)+e^{i\theta_1}\sin\left(\frac{2k\pi}{N+1}\right)+e^{i(\theta_1+\theta_2)}\sin\left(\frac{3k\pi}{N+1}\right)+\cdots \\
&+e^{i\sum_{\nu=1}^{N-3}\theta_\nu}\sin\left(\frac{N-2}{N+1}k\pi\right)+e^{i\sum_{\nu=1}^{N-2}\theta_\nu}\sin\left(\frac{N-1}{N+1}k\pi\right)+e^{i\sum_{\nu=1}^{N-1}\theta_\nu}\sin\left(\frac{Nk\pi}{N+1}\right)\Bigg] \\
=\;& \frac{G}{A}\Bigg\{\left[\sin\left(\frac{1}{N+1}k\pi\right)+e^{i\sum_{\nu=1}^{N-1}\theta_\nu}\sin\left(\frac{N}{N+1}k\pi\right)\right]+\left[e^{i\theta_1}\sin\left(\frac{2}{N+1}k\pi\right)+e^{i\sum_{\nu=1}^{N-2}\theta_\nu}\sin\left(\frac{N-1}{N+1}k\pi\right)\right] \\
&+\left[e^{i(\theta_1+\theta_2)}\sin\left(\frac{3}{N+1}k\pi\right)+e^{i\sum_{\nu=1}^{N-3}\theta_\nu}\sin\left(\frac{N-2}{N+1}k\pi\right)\right]+\cdots\Bigg\}. \qquad \text{(S86)}
\end{aligned}$$

Below, we consider two cases corresponding to odd and even numbers N, respectively.

(i) For an odd number N and $\theta_j = 0$ (for j = 2-$(N-1)$), the coefficient becomes

$$\begin{aligned}
&\frac{G}{A}\left[\sin\left(\frac{k\pi}{N+1}\right)+\sum_{j=2}^{N} e^{i\sum_{\nu=1}^{j-1}\theta_\nu}\sin\left(\frac{jk\pi}{N+1}\right)\right] \\
=\;& \frac{G}{A}\Bigg\{\left[\sin\left(\frac{k\pi}{N+1}\right)+e^{i\theta_1}\sin\left(\frac{Nk\pi}{N+1}\right)\right]+e^{i\theta_1}\left[\sin\left(\frac{2k\pi}{N+1}\right)+\sin\left(\frac{N-1}{N+1}k\pi\right)\right] \\
&+e^{i\theta_1}\left[\sin\left(\frac{3k\pi}{N+1}\right)+\sin\left(\frac{N-2}{N+1}k\pi\right)\right]+\cdots+e^{i\theta_1}\sin\left(\frac{k\pi}{2}\right)\Bigg\}. \qquad \text{(S87)}
\end{aligned}$$

On one hand, if k is an odd number, we have

$$\begin{aligned}
&\frac{G}{A}\left[\sin\left(\frac{k\pi}{N+1}\right)+\sum_{j=2}^{N} e^{i\sum_{\nu=1}^{j-1}\theta_\nu}\sin\left(\frac{jk\pi}{N+1}\right)\right] \\
=\;& \frac{G}{A}\left[(1+e^{i\theta_1})\sin\left(\frac{k\pi}{N+1}\right)+2e^{i\theta_1}\sin\left(\frac{2k\pi}{N+1}\right)+2e^{i\theta_1}\sin\left(\frac{3k\pi}{N+1}\right)+\cdots+e^{i\theta_1}\sin\left(\frac{k\pi}{2}\right)\right]; \qquad \text{(S88)}
\end{aligned}$$

On the other hand, if k is an even number, we have

$$\frac{G}{A}\left[\sin\left(\frac{k\pi}{N+1}\right)+\sum_{j=2}^{N} e^{i\sum_{\nu=1}^{j-1}\theta_\nu}\sin\left(\frac{jk\pi}{N+1}\right)\right]=\frac{G}{A}\left(1-e^{i\theta_1}\right)\sin\left(\frac{k\pi}{N+1}\right). \qquad \text{(S89)}$$

(ii) For an even number N and $\theta_j = 0$ (for j = 2-$(N-1)$), the coefficient can be simplified as

$$\begin{aligned}
&\frac{G}{A}\left[\sin\left(\frac{k\pi}{N+1}\right)+\sum_{j=2}^{N} e^{i\sum_{\nu=1}^{j-1}\theta_\nu}\sin\left(\frac{jk\pi}{N+1}\right)\right] \\
=\;& \frac{G}{A}\Bigg\{\left[\sin\left(\frac{k\pi}{N+1}\right)+e^{i\theta_1}\sin\left(\frac{N}{N+1}k\pi\right)\right]+e^{i\theta_1}\left[\sin\left(\frac{2k\pi}{N+1}\right)+\sin\left(\frac{N-1}{N+1}k\pi\right)\right] \\
&+e^{i\theta_1}\left[\sin\left(\frac{3k\pi}{N+1}\right)+\sin\left(\frac{N-2}{N+1}k\pi\right)\right]+\cdots\Bigg\}. \qquad \text{(S90)}
\end{aligned}$$

In this case, when k is an odd number, we have

$$\begin{aligned}
&\frac{G}{A}\left[\sin\left(\frac{k\pi}{N+1}\right)+\sum_{j=2}^{N} e^{i\sum_{\nu=1}^{j-1}\theta_\nu}\sin\left(\frac{jk\pi}{N+1}\right)\right] \\
=\;& \frac{G}{A}\left[(1+e^{i\theta_1})\sin\left(\frac{k\pi}{N+1}\right)+2e^{i\theta_1}\sin\left(\frac{2k\pi}{N+1}\right)+2e^{i\theta_1}\sin\left(\frac{3k\pi}{N+1}\right)+\cdots\right]; \qquad \text{(S91)}
\end{aligned}$$

In addition, when k is an even number, we have

$$\frac{G}{A}\left[\sin\left(\frac{k\pi}{N+1}\right)+\sum_{j=2}^{N}e^{i\sum_{\nu=1}^{j-1}\theta_\nu}\sin\left(\frac{jk\pi}{N+1}\right)\right]=\frac{G}{A}\left(1-e^{i\theta_1}\right)\sin\left(\frac{k\pi}{N+1}\right). \tag{S92}$$

According to Eqs. (S87-S92), we can see that for odd numbers k, the coupling strength between the cavity-field mode and the kth normal mode B_k is nonzero. However, for even numbers k, the coupling strength between the cavity-field mode and the kth normal mode B_k can be expressed as

$$H_{\rm ck}=\frac{G}{A}\left[\left(1-e^{i\theta_1}\right)\sin\left(\frac{k\pi}{N+1}\right)\right]aB_k^\dagger+\text{H.c.},\qquad k=\text{even number}. \tag{S93}$$

Obviously, when $\theta_1=2n\pi$, the coupling strength between the kth mechanical normal mode ($B_{k=\text{even}}$) and the cavity mode (a) is equal to zero. In this case, all the even normal modes are decoupled from the cavity field. Then ground-state cooling cannot be realized in this system due to the dark-mode effect. Nevertheless, we can cool these mechanical resonators by choosing proper parameters to break the dark-mode effect ($\theta_1\neq 2n\pi$).

VI. GROUND-STATE COOLING OF THE MULTIPLE MECHANICAL RESONATORS

In this section, we study the simultaneous cooling of multiple mechanical resonators in the N-mechanical-resonator optomechanical system. To evaluate the cooling performance of the multiple mechanical resonators, we calculate the final average phonon numbers in these mechanical resonators. To this end, we re-express the linearized quantum Langevin equations (S75) as

$$\dot{\mathbf{u}}(t)=\mathbf{A}\mathbf{u}(t)+\mathbf{N}(t), \tag{S94}$$

where we introduce the vectors of the system operators

$$\mathbf{u}(t)=[\delta a(t),\delta b_1(t),\delta b_2(t),\cdots,\delta b_N(t),\delta a^\dagger(t),\delta b_1^\dagger(t),\delta b_2^\dagger(t),\cdots,\delta b_N^\dagger(t)]^T, \tag{S95}$$

the vector of the noise operators

$$\mathbf{N}(t)=\sqrt{2}[\sqrt{\kappa}a_{\rm in}(t),\sqrt{\gamma_1}b_{1,\rm in}(t),\sqrt{\gamma_2}b_{2,\rm in}(t),\cdots,\sqrt{\gamma_N}b_{N,\rm in}(t),\sqrt{\kappa}a_{\rm in}^\dagger(t),\sqrt{\gamma_1}b_{1,\rm in}^\dagger(t),\sqrt{\gamma_2}b_{2,\rm in}^\dagger(t),\cdots,\sqrt{\gamma_N}b_{N,\rm in}^\dagger(t)]^T, \tag{S96}$$

and the coefficient matrix

$$\mathbf{A}=\begin{pmatrix}
-(\kappa+i\Delta) & -iG_1 & -iG_2 & \cdots & -iG_N & 0 & -iG_1 & -iG_2 & \cdots & -iG_N\\
-iG_1^* & -(\gamma_1+i\omega_1) & -i\eta_1e^{i\theta_1} & \cdots & -i\eta_{N-1}e^{-i\theta_{N-1}} & -iG_1 & 0 & 0 & \cdots & 0\\
-iG_2^* & -i\eta_1e^{-i\theta_1} & -(\gamma_2+i\omega_2) & \cdots & 0 & -iG_2 & 0 & 0 & \cdots & 0\\
\vdots & \vdots & \vdots & \ddots & \vdots & \vdots & \vdots & \vdots & \ddots & \vdots\\
-iG_N^* & -i\eta_{N-1}e^{i\theta_{N-1}} & 0 & \cdots & -(\gamma_N+i\omega_N) & -iG_4 & 0 & 0 & \cdots & 0\\
0 & iG_1^* & iG_2^* & \cdots & iG_N^* & -(\kappa-i\Delta) & iG_1^* & iG_2^* & \cdots & iG_N^*\\
iG_1^* & 0 & 0 & \cdots & 0 & iG_1 & -(\gamma_1-i\omega_1) & i\eta_1e^{-i\theta_1} & \cdots & i\eta_{N-1}e^{i\theta_{N-1}}\\
iG_2^* & 0 & 0 & \cdots & 0 & iG_2 & i\eta_1e^{i\theta_1} & -(\gamma_2-i\omega_2) & \cdots & 0\\
\vdots & \vdots & \vdots & \vdots & \vdots & \vdots & \vdots & \vdots & \ddots & \vdots\\
iG_N^* & 0 & 0 & \cdots & 0 & iG_N & i\eta_{N-1}e^{-i\theta_{N-1}} & 0 & \cdots & -(\gamma_N-i\omega_N)
\end{pmatrix}. \tag{S97}$$

The formal solution of the linearized quantum Langevin equations Eq. (S94) can be obtained as

$$\mathbf{u}(t)=\mathbf{M}(t)\mathbf{u}(0)+\int_0^t\mathbf{M}(t-s)\mathbf{N}(s)ds, \tag{S98}$$

where the matrix $\mathbf{M}(t)$ is given by $\mathbf{M}(t)=\exp(\mathbf{A}t)$, and hence the stability conditions derived from the Routh-Hurwitz criterion have satisfied. Note that in our simulations the real part of the eigenvalues of the coefficient matrix $\mathbf{A}$ is negative.

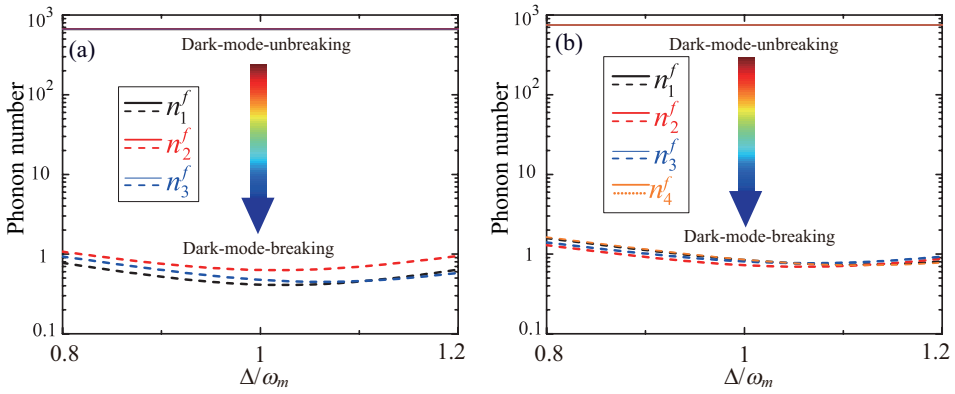

FIG. S10: (Color online) The final average phonon numbers n_j^f in these mechanical resonators as functions of the effective driving detuning Δ in the dark-mode-unbreaking case ($\eta_j = \eta = 0$) and the dark-mode-breaking case ($\eta_j/\omega_m = \eta/\omega_m = 0.1$, $\theta_1 = \pi/2$, and $\theta_{j\neq 1} = 0$) for $N = 3$ and $N = 4$. Here we take $G_j/\omega_m = G/\omega_m = 0.1$, $\kappa/\omega_m = 0.2$, $\gamma_j/\omega_m = 10^{-5}$, and $\bar{n}_j = 10^3$.

For studying the quantum cooling of these mechanical resonators, we calculate the steady-state average phonon numbers in these mechanical resonators. This can be realized by calculating the steady-state values of the covariance matrix $\mathbf{V}$, which is defined by the matrix elements

$$\mathbf{V}_{ij} = \frac{1}{2}[\langle \mathbf{u}_i(\infty)\mathbf{u}_j(\infty)\rangle + \langle \mathbf{u}_j(\infty)\mathbf{u}_i(\infty)\rangle]. \tag{S99}$$

In the linearized optomechanical system, the covariance matrix $\mathbf{V}$ satisfies the Lyapunov equation

$$\mathbf{A}\mathbf{V} + \mathbf{V}\mathbf{A}^T = -\mathbf{Q}, \tag{S100}$$

where

$$\mathbf{Q} = \frac{1}{2}(\mathbf{C} + \mathbf{C}^T). \tag{S101}$$

Here $\mathbf{C}$ is the noise correlation matrix which is defined by the elements

$$\langle \mathbf{N}_k(s)\mathbf{N}_l(s')\rangle = \mathbf{C}_{k,l}\delta(s - s'). \tag{S102}$$

For the Markovian baths as considered in this work, we have $\mathbf{C}(s, s') = \mathbf{C}\delta(s - s')$, where the constant matrix $\mathbf{C}$ is given by

$$\mathbf{C} = \begin{pmatrix} 0 & 0 & 0 & \cdots & 0 & 2\kappa & 0 & 0 & \cdots & 0 \\ 0 & 0 & 0 & \cdots & 0 & 0 & 2\gamma_1(\bar{n}_1+1) & 0 & \cdots & 0 \\ 0 & 0 & 0 & \cdots & 0 & 0 & 0 & 2\gamma_2(\bar{n}_2+1) & \cdots & 0 \\ \vdots & \vdots & \vdots & \vdots & \vdots & \vdots & \vdots & \vdots & \ddots & 0 \\ 0 & 0 & 0 & \cdots & 0 & 0 & 0 & 0 & \cdots & 2\gamma_N(\bar{n}_N+1) \\ 0 & 0 & 0 & \cdots & 0 & 0 & 0 & 0 & \cdots & 0 \\ 0 & 2\gamma_1\bar{n}_1 & 0 & \cdots & 0 & 0 & 0 & 0 & \cdots & 0 \\ 0 & 0 & 2\gamma_2\bar{n}_2 & \cdots & 0 & 0 & 0 & 0 & \cdots & 0 \\ \vdots & \vdots & \vdots & \ddots & \vdots & \vdots & \vdots & \vdots & \ddots & \vdots \\ 0 & 0 & 0 & \cdots & 2\gamma_N\bar{n}_N & 0 & 0 & 0 & \cdots & 0 \end{pmatrix}. \tag{S103}$$

Based on the covariance matrix $\mathbf{V}$, the final average phonon number in the jth mechanical resonator can be obtained as

$$\langle \delta b_j^\dagger \delta b_j\rangle = \mathbf{V}_{N+j+2,j+1} - \frac{1}{2}, \tag{S104}$$

where $\mathbf{V}_{N+j+2,j+1}$ can be obtained by solving the Lyapunov equation.

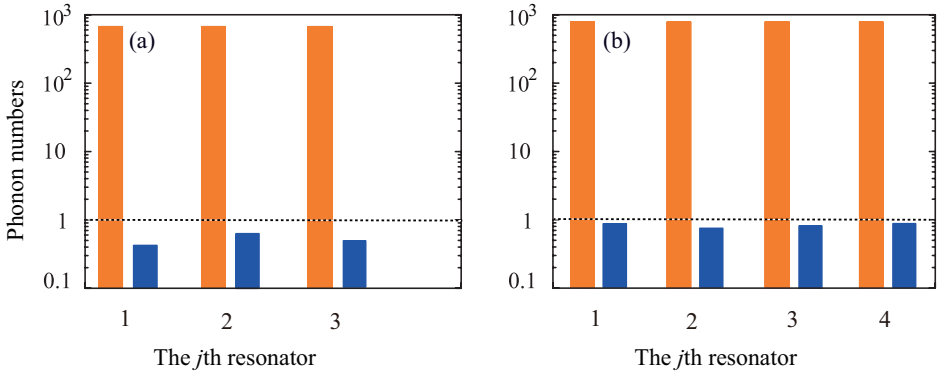

FIG. S11: (Color online) The final average phonon numbers n_j^f in these mechanical resonators are plotted in the dark-mode-unbreaking [$\eta_j = 0$ (orange bars)] and -breaking [$\eta_j = 0.1\omega_m$ and $\theta_1 = \pi/2$ (blue bars)] cases for (a) $N = 3$ and (b) $N = 4$. Here $\Delta = \omega_m$, and other used parameters are the same as those given in Fig. S10.

Below we simulate the cooling performance of the mechanical resonators for the cases of $N = 3$ and 4. For convenience, we assume that all the mechanical resonators have the same resonance frequencies ($\omega_j = \omega_m$ for $j = 1$-N), optomechanical coupling strengths ($G_j = G$ for $j = 1$-N), and phonon-exchange coupling strengths [$\eta_j = \eta$ for $j = 1$-$(N-1)$]. Moreover, we consider the case of $\theta_1 = \pi/2$ and $\theta_{j>2} = 0$. In Fig. S10, we plot the final average phonon numbers n_j^f in these mechanical resonators as functions of the scaled driving detuning Δ/ω_m in both the dark-mode-breaking ($\eta_j = 0.1\omega_m$ and $\theta_1 = \pi/2$) and -unbreaking ($\eta_j = \eta = 0$) cases. The results show that the ground-state cooling is unfeasible for these mechanical resonators when the phonon-exchange interactions are absent ($\eta_j = \eta = 0$) [the upper curves in Figs. S10(a) and S10(b)]. This is because the phonon excitation energy stored in the dark modes cannot be extracted through the optomechanical cooling channel. When the couplings among these mechanical resonators are introduced, the dark modes are broken and then the ground-state cooling can be realized, as shown in Figs. S10(a) and S10(b). In particular, the optimal driving detuning is located at $\Delta \approx \omega_m$, in consistent with the resolved-sideband cooling case.

To see the cooling performance more clearly, we compare the cooling results of these mechanical resonators in the presence of mechanical couplings with the results corresponding to the absence of the mechanical couplings. In Fig. S11, we plot the final average phonon numbers of these mechanical resonators in the two cases. Here we can see that final average phonon numbers could be smaller than 1 when the mechanical couplings are introduced into the system, which means that the simultaneous ground-state cooling of these mechanical resonators can be achieved by breaking the dark-mode effect.

We also investigate the dependence of the cooling performance on the mechanical coupling parameters η and θ. In Fig. S12, we plot the final average phonon numbers n_j^f in these mechanical resonators as functions of the phase θ and

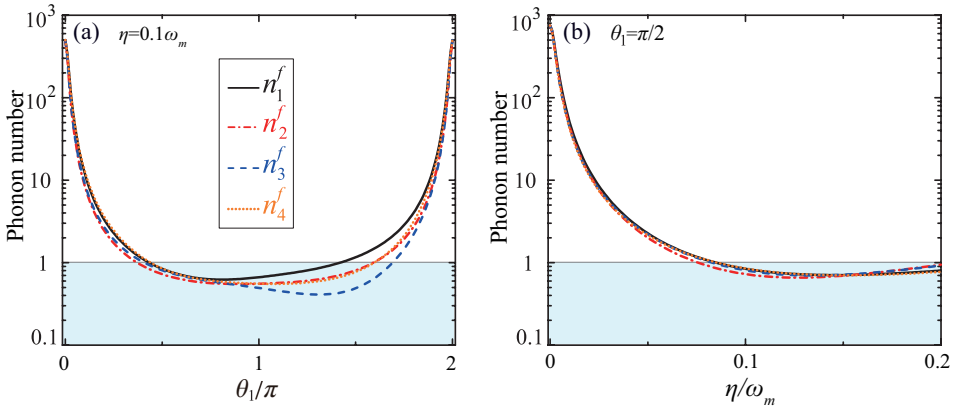

FIG. S12: (Color online) The final average phonon numbers n_j^f in the mechanical resonators as functions of (a) the phase θ_1 when $\eta/\omega_m = 0.1$ and (b) the phonon-exchange coupling η when $\theta_1 = \pi/2$ for $N = 4$. Here $G_j/\omega_m = G/\omega_m = 0.1$. Other used parameters are the same as those given in Fig. S10.

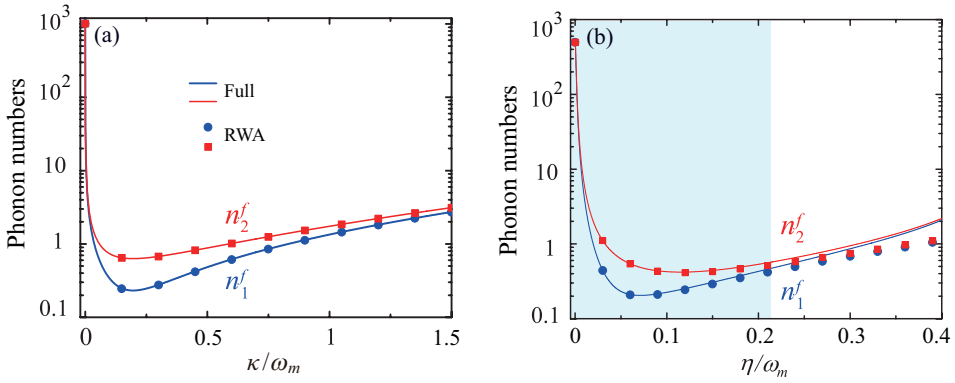

FIG. S13: (Color online) The final average phonon numbers n_1^f and n_2^f versus (a) the cavity-field decay rate κ when $\eta = 0.05\omega_m$ and (b) the phonon-phonon coupling strength η when $\kappa = 0.2\omega_m$. Here the symbols and the solid curves correspond to the Hamiltonian under the RWA and the full Hamiltonian, respectively. Other parameters used are given by $\omega_2 = \omega_1 = \omega_m$, $\Delta = \omega_m$, $\theta = \pi/2$, $G_1 = G_2 = 0.1\omega_m$, $\gamma_1 = \gamma_2 = 10^{-5}\omega_m$, and $\bar{n}_1 = \bar{n}_2 = 10^3$.

the scaled phonon-exchange coupling strength η/ω_m. The results show that ground-state cooling can be realized for proper values of the phase $\theta_1 \neq 2n\pi$ when $\eta = 0.1\omega_m$ [Fig. S12(a)]. In addition, the cooling efficiency of the multiple mechanical resonators can be controlled by tuning the phonon-exchange interaction strength η when the phase is fixed at $\theta_1 = \pi/2$ [Fig. S12(b)]. Under these parameters, the dark-mode effect is broken and then the thermal occupations can be extracted through the optomechanical-cooling channels.

VII. DISCUSSIONS ON THE JUSTIFICATION OF PERFORMING THE RWA

In our model, we consider an excitation-number-conservation-type phonon-phonon interaction $\eta(e^{i\theta}b_1^\dagger b_2 + e^{-i\theta}b_2^\dagger b_1)$, which is obtained by making the rotating-wave approximation (RWA) in the full phonon-exchange interaction Hamiltonian $\eta(e^{i\theta}b_1^\dagger + e^{-i\theta}b_1)(b_2^\dagger + b_2)$. To evaluate the validity of the RWA, we compare the results obtained based on the approximate Hamiltonian and the full Hamiltonian including the counterrotating term. In Figs. S13(a) and S13(b), we show the final average phonon numbers n_1^f and n_2^f as functions of the cavity-field decay rate κ and the mechanical coupling strength η. Here, the symbols and the solid curves correspond to the Hamiltonian under the RWA and the full Hamiltonian, respectively. Figure S13(a) shows an excellent agreement between the results obtained with the approximate Hamiltonian and the full Hamiltonian in both the resolved- and unresolved-sideband regimes. We can also see from Fig. S13(b) that the approximate results match well with the exact results when $\eta < 0.2\omega_m$. Physically, the optomechanical cooling and heating are governed by the rotating-wave and the CR terms, respectively. In the weak-coupling regime ($\eta \ll \omega_m$) and under the near-resonance condition (ω_2 around ω_1), the CR term in the phonon-phonon interaction can be safely omitted by applying the RWA. The difference between these two treatments becomes non-negligible when $\eta > 0.2\omega_m$. The reason is that the CR term, which simultaneously creates phonon excitations in the two mechanical resonators, becomes important for a large phonon-phonon coupling strength η. These features indicate that the RWA performed in the phonon-phonon interaction is justified in our simulations, and that the CR interaction can be omitted safely under the condition $\eta \ll \omega_m$.

VIII. SIMULTANEOUS COOLING OF THE MECHANICAL SUPERMODES

In this section, we discuss the simultaneous cooling of the mechanical supermodes in cavity optomechanical systems. Note that the notations used in this section are independent of the those used in other sections. We consider the case where the two mechanical resonators are coupled to each other by a phonon-hopping coupling. Then, two mechanical supermodes are formed and the cavity field is coupled to the two supermodes. In the presence of the phonon-hopping coupling between the two mechanical resonators, the Hamiltonian of this coupled mechanical system reads ($\hbar = 1$)

$$H_c = \omega_m c_1^\dagger c_1 + \omega_m c_2^\dagger c_2 + \lambda(c_1^\dagger c_2 + c_2^\dagger c_1), \tag{S105}$$

where the operators $c_{l=1,2}$ ($c_l^\dagger$) are the annihilation (creation) operators of the lth mechanical resonator, with the corresponding resonance frequencies ω_m, and the parameter λ is a coupling constant of the mechanical interaction

between the two mechanical resonators. In the weak-coupling regime ($\lambda \ll \omega_m$), the counter-rotating term in the phonon-phonon interaction can be safely omitted by making the rotating-wave approximation. Below, we diagonalize this coupled mechanical system by introducing two mechanical supermodes $C_\pm$, given by

$$C_+ = \frac{1}{\sqrt{2}}(c_1 + c_2), \tag{S106a}$$

$$C_- = \frac{1}{\sqrt{2}}(-c_1 + c_2), \tag{S106b}$$

where these new operators satisfy the bosonic commutation relations $[C_+, C_+^\dagger] = 1$ and $[C_-, C_-^\dagger] = 1$. Thus, Hamiltonian (S105) becomes

$$H_c = \omega_{C,+} C_+^\dagger C_+ + \omega_{C,-} C_-^\dagger C_-, \tag{S107}$$

where we introduce the resonance frequencies of these supermodes as

$$\omega_{C,\pm} = \omega_m \pm \lambda. \tag{S108}$$

To cool the two mechanical supermodes, we couple the two mechanical supermodes to a common optical cavity-field mode by the optomechanical interactions [S1]. In the strong-driving regime, the linearized optomechanical Hamiltonian in the RWA takes the form as

$$H_{\rm RWA} = \Delta \delta a^\dagger \delta a + \omega_{C,+} \delta C_+^\dagger \delta C_+ + \omega_{C,-} \delta C_-^\dagger \delta C_- + G_+(\delta a \delta C_+^\dagger + \delta a^\dagger \delta C_+) + G_-(\delta a \delta C_-^\dagger + \delta a^\dagger \delta C_-), \tag{S109}$$

where Δ is the normalized driving detuning of the cavity field, and the parameters $G_\pm$ are the optomechanical couplings between the cavity-field mode and the two mechanical supermodes. It can be seen from Eq. (S109) that the couplings between the cavity field and the two supermodes are the same as the three-mode optomechanical model considered in the main text. Therefore, all the analyses in the three-mode optomechanical system are suitable to the coupled cavity-supermode case. Based on the fact that the mechanical coupling between the two mechanical resonators is much smaller than the resonant frequencies of the two resonators ($\lambda \ll \omega_m$), the frequencies $\omega_{C,\pm}$ of the two mechanical supermodes are close to each other. We proceed to analyze the cooling performance of the two mechanical supermodes. Concretely, we consider two special cases.

(i) When the frequency difference between the two mechanical supermodes is larger than the effective mechanical linewidth ($\Delta\omega = |\omega_{C,+} - \omega_{C,-}| > \Gamma_{l=+,-}$), the simultaneous ground-state cooling of the two mechanical supermodes is accessible under proper parameter conditions. Physically, when the two mechanical supermodes are well separated in frequency, there is no dark mode, then the ground-state cooling can be realized when this system works in the resolved-sideband regime and under a proper driving (red-sideband resonance). This cooling situation is similar to the case shown in Fig. 2(b) and Fig. S1(e) [see blank area].

(ii) When the frequency difference between the two mechanical supermodes is smaller than the effective mechanical linewidth ($\Delta\omega = |\omega_{C,+} - \omega_{C,-}| \leq \Gamma_{l=+,-}$), the cooling of the two mechanical supermodes is suppressed. This is because, though the dark mode exists theoretically only in the degenerate-resonator case, the dark-mode effect actually works for a wider detuning range in the near-degenerate-resonator case. The suppression region of the ground-state for the mechanical supermodes is characterized by the effective mechanical linewidth. The cooling of the individual mechanical supermodes is suppressed in this region, i.e., the individual mechanical supermodes have significant spectral overlap and become effectively degenerate. This cooling situation is similar to the case shown in Fig. 2(b) and Fig. S1(e) [see shadow area].

In the case (ii), for achieving quantum ground-state cooling of the two mechanical supermodes, we need to introduce a phase-dependent phonon-hopping coupling between the two mechanical supermodes. Thus, the linearized optomechanical Hamiltonian including a phase-dependent coupling between the two supermodes takes the following form

$$\begin{aligned} H_{\rm RWA} = {} & \Delta \delta a^\dagger \delta a + \omega_{C,+} \delta C_+^\dagger \delta C_+ + \omega_{C,-} \delta C_-^\dagger \delta C_- + G_+(\delta a \delta C_+^\dagger + \delta a^\dagger \delta C_+) + G_-(\delta a \delta C_-^\dagger + \delta a^\dagger \delta C_-) \\ & + \tilde{\lambda}(e^{i\phi} \delta C_+^\dagger \delta C_- + e^{-i\phi} \delta C_-^\dagger \delta C_+). \end{aligned} \tag{S110}$$

By introducing two new bosonic modes $\tilde{C}_+$ and $\tilde{C}_-$ defined by

$$\tilde{C}_+ = \tilde{f}' C_+ - e^{i\phi} \tilde{h}' C_-, \tag{S111a}$$

$$\tilde{C}_- = e^{-i\phi} \tilde{h}' C_+ + \tilde{f}' C_-, \tag{S111b}$$

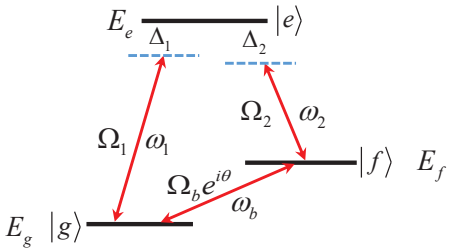

FIG. S14: Schematic diagram of the three-level system with these states $|g\rangle$, $|f\rangle$, and $|e\rangle$ (with the corresponding energies E_g, E_f, and E_e). A Lambda-type coupling configuration is formed by the transition processes $|g\rangle \to |e\rangle$ and $|f\rangle \to |e\rangle$ with the coupling strengthes Ω_1 and Ω_2, and the detunings Δ_1 and Δ_2. A phase-dependent resonant coupling (with the coupling strength $\Omega_b e^{i\theta}$) between the two lower states $|g\rangle$ and $|f\rangle$ is introduced to break the dark-state effect existing in the Lambda-type three-level system working in the two-photon resonance regime $\Delta_1 = \Delta_2 = \Delta$.

Hamiltonian (S110) becomes

$$H_{\rm RWA} = \Delta\delta a^\dagger \delta a + \tilde{\omega}_{C,+}\tilde{C}_+^\dagger \tilde{C}_+ + \tilde{\omega}_{C,-}\tilde{C}_-^\dagger \tilde{C}_- + \tilde{G}_+(\delta a \tilde{C}_+^\dagger + \delta a^\dagger \tilde{C}_+) + \tilde{G}_-(\delta a \tilde{C}_-^\dagger + \delta a^\dagger \tilde{C}_-), \tag{S112}$$

where we introduce the resonance frequencies $\tilde{\omega}_{C,\pm}$, the coupling strengths $\tilde{G}_\pm$, and the coefficients $\tilde{f}'$ and $\tilde{h}'$ as

$$\tilde{\omega}_{C,+} = \frac{1}{2}\left(\omega_{C,+} + \omega_{C,-} + \sqrt{(\omega_{C,+} - \omega_{C,-})^2 + 4\tilde{\lambda}^2}\right), \tag{S113a}$$

$$\tilde{\omega}_{C,-} = \frac{1}{2}\left(\omega_{C,+} + \omega_{C,-} - \sqrt{(\omega_{C,+} - \omega_{C,-})^2 + 4\tilde{\lambda}^2}\right), \tag{S113b}$$

$$\tilde{G}_+ = (\tilde{f}' G_+ - e^{-i\phi}\tilde{h}' G_-), \tag{S113c}$$

$$\tilde{G}_- = (e^{i\phi}\tilde{h}' G_+ + \tilde{f}' G_-), \tag{S113d}$$

with

$$\tilde{f}' = \frac{|\tilde{\omega}_{C,-} - \omega_{C,+}|}{\sqrt{(\tilde{\omega}_{C,-} - \omega_{C,+})^2 + \tilde{\lambda}^2}}, \tag{S114a}$$

$$\tilde{h}' = \frac{\tilde{\lambda}}{(\tilde{\omega}_{C,-} - \omega_{C,+})}\tilde{f}'. \tag{S114b}$$

We note that the cooling of the two mechanical supermodes can also be explained by the physical mechanism proposed in this manuscript. By combining this phase-dependent phonon-exchange interaction with the optomechanical couplings, the interference effect works and the dark-mode effect is broken, which can lead to the ground-state cooling of the two mechanical supermodes.

IX. PHYSICAL MECHANISM FOR BREAKING THE DARK-STATE EFFECT IN A LAMBDA-TYPE THREE-LEVEL SYSTEM

In this section, we show the physical mechanism for breaking the dark-state effect in a Lambda-type three-level system by introducing a phase-dependent transition between the two lower levels (as shown in Fig. S14). It is well known that there exists a dark state in the Lambda-type three-level system in the two-photon resonance regime. For the dark state, the superposition coefficient of the excited state is zero. Below, we show that this dark state will be broken by introducing a phase-dependent transition coupling between the two lower states. Note that in a typical natural atom, the direct transition between the two lower states of a Lambda three-level atom is forbidden due to the transition selection rule. However, this transition is accessible either in artificial cycle three-level systems [S2] or induced by indirect transition. The Hamiltonian of the system reads

$$\begin{aligned} H \;=\; & E_e|e\rangle\langle e| + E_f|f\rangle\langle f| + E_g|g\rangle\langle g| + \Omega_1(|e\rangle\langle g|e^{-i\omega_1 t} + |g\rangle\langle e|e^{i\omega_1 t}) + \Omega_2(|e\rangle\langle f|e^{-i\omega_2 t} + |f\rangle\langle e|e^{i\omega_2 t}) \\ & + \Omega_b(|f\rangle\langle g|e^{i\theta}e^{-i\omega_b t} + |g\rangle\langle f|e^{-i\theta}e^{i\omega_b t}), \end{aligned} \tag{S115}$$

where E_e, E_f, and E_g are, respectively, the energies of these three energy levels $|e\rangle$, $|f\rangle$, and $|g\rangle$. Two monochromatic fields with frequencies ω_1 and ω_2 are coupled to the atomic transitions $|g\rangle \to |e\rangle$ and $|f\rangle \to |e\rangle$ (forming a Lambda configuration of couplings), respectively, with Ω_1 and Ω_2 being the corresponding real transition amplitudes. In this system, corresponding to these two transitions $|g\rangle \to |e\rangle$ and $|f\rangle \to |e\rangle$, we introduce the transition detunings as $\Delta_1 = E_e - E_g - \omega_1$ and $\Delta_2 = E_e - E_f - \omega_2$. We know that the Labmda-type couplings support a dark state in this system when the transitions satisfy the two-photon resonance condition [$\Delta_1 = \Delta_2$ in Fig. S14]. Below, we will focus on the two-photon resonant transition case, $\Delta_1 = \Delta_2 = \Delta$. To exhibit our dark-state-breaking idea, we introduce a field to resonantly couple the two lower states $|f\rangle$ and $|g\rangle$. In particular, this coupling has a phase-dependent coupling strength, which is the critical factor for this dark-state-breaking approach. In a rotating frame with respect to

$$H_0 = (E_g + \omega_1)|e\rangle\langle e| + E_f|f\rangle\langle f| + E_g|g\rangle\langle g|, \tag{S116}$$

the Hamiltonian of the system becomes

$$V_I = \Delta|e\rangle\langle e| + \Omega_1(|e\rangle\langle g| + |g\rangle\langle e|) + \Omega_2(|e\rangle\langle f| + |f\rangle\langle e|) + \Omega_b(|f\rangle\langle g|e^{i\theta} + |g\rangle\langle f|e^{-i\theta}). \tag{S117}$$

By defining these three basis states with the following vectors

$$|e\rangle = (1,0,0)^T, \quad |f\rangle = (0,1,0)^T, \quad |g\rangle = (0,0,1)^T, \tag{S118}$$

where "T" denotes the matrix transpose, the interaction Hamiltonian V_I can be expressed as

$$V_I = \begin{pmatrix} \Delta & \Omega_2 & \Omega_1 \\ \Omega_2 & 0 & \Omega_b e^{i\theta} \\ \Omega_1 & \Omega_b e^{-i\theta} & 0 \end{pmatrix}. \tag{S119}$$

For the sake of simplicity and without loss of generality, we consider the symmetric coupling case $\Omega_1 = \Omega_2 = \Omega$ and the single- and two-photon resonance case $\Delta_1 = \Delta_2 = \Delta = 0$, then the Hamiltonian (S119) becomes

$$V_I = \Omega \begin{pmatrix} 0 & 1 & 1 \\ 1 & 0 & \eta e^{i\theta} \\ 1 & \eta e^{-i\theta} & 0 \end{pmatrix}, \tag{S120}$$

where we introduce the ratio $\eta = \Omega_b/\Omega$.

The dark-state effect can be analyzed by investigating the eigensystem of the matrix V_I in Eq. (S120). The eigen-equation can be expressed as

$$\frac{1}{\Omega} V_I|\lambda_s\rangle = \lambda_s|\lambda_s\rangle, \quad s = 1,2,3, \tag{S121}$$

where λ_s are the eigenvalues, which are determined by the secular (cubic) equation

$$\lambda^3 - (2+\eta^2)\lambda - 2\eta\cos\theta = 0. \tag{S122}$$

Using the Cardano formula, the solutions of the cubic equation (S122) can be obtained as

$$\lambda_1 = s_1 + s_2, \quad \lambda_2 = -\frac{1}{2}(s_1+s_2) + \frac{i\sqrt{3}}{2}(s_1 - s_2), \quad \lambda_3 = -\frac{1}{2}(s_1+s_2) - \frac{i\sqrt{3}}{2}(s_1 - s_2), \tag{S123}$$

where

$$s_1 = \left(r + \sqrt{q^3 + r^2}\right)^{\frac{1}{3}}, \quad s_2 = \left(r - \sqrt{q^3 + r^2}\right)^{\frac{1}{3}}, \tag{S124}$$

with $q = -(2+\eta^2)/3$ and $r = \eta\cos\theta$.

In general, the form of these eigenstates defined in Eq. (S121) can be expressed as

$$|\lambda_s\rangle = c_g^{[s]}|g\rangle + c_f^{[s]}|f\rangle + c_e^{[s]}|e\rangle, \quad s = 1,2,3. \tag{S125}$$

The dark state can be checked by calculating the probability of the excited state $|e\rangle$ in these eigenstates as follows

$$P_e^{[s]} = |\langle e|\lambda_s\rangle|^2 = |c_e^{[s]}|^2, \quad s = 1,2,3. \tag{S126}$$

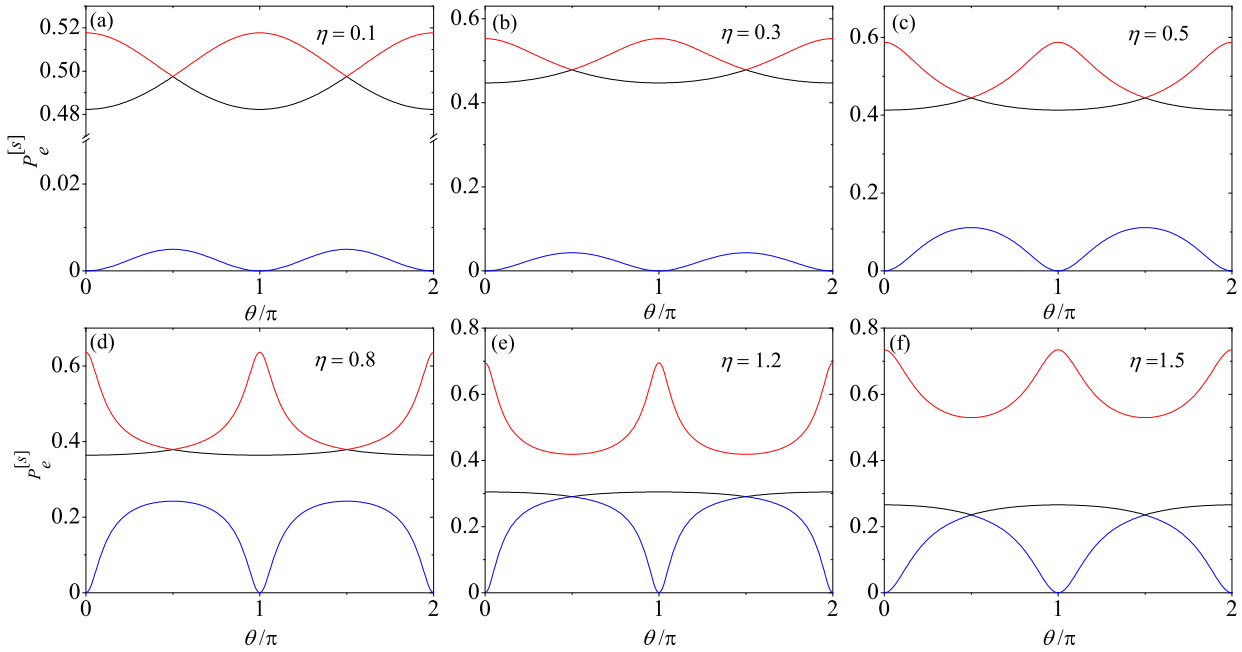

FIG. S15: The probability $P_e^{[s]}$ of the excited state $|e\rangle$ in these eigenstates $|\lambda_s\rangle$ as a function of θ when (a) $\eta = \Omega_b/\Omega = 0.1$, (b) 0.3, (c) 0.5, (d) 0.8, (e) 1.2, and (f) 1.5. Here, we can see that one of these three eigenstates has no excited state probability at $\theta = n\pi$, which means that there is a dark state at $\theta = n\pi$ and hence the dark-state effect is broken when $\theta \neq n\pi$.

The case $P_e^{[s]} = 0$ implies a dark state of this system. In Fig. S15, we plot the probability $P_e^{[s]}$ of the excited state $|e\rangle$ in these three eigenstates $|\lambda_s\rangle$ as a function of θ when the ratio $\eta = \Omega_b/\Omega$ takes various values. Here we can see that when $\theta = n\pi$ for an integer n, one of the eigenstates becomes a dark state. In other cases, there are no dark states. Therefore, the phase-dependent resonant transition $|g\rangle \leftrightarrow |f\rangle$ can be used to break the dark-state effect in this Lambda-type three-level system.

The analytical expressions of these eigenstates can be obtained as

$$|\lambda_s\rangle = \Lambda_s \left[|g\rangle + \frac{\lambda_s \eta e^{i\theta} + 1}{\lambda_s^2 - 1}|f\rangle + \frac{\eta e^{i\theta} + \lambda_s}{\lambda_s^2 - 1}|e\rangle \right], \qquad s = 1, 2, 3, \tag{S127}$$

where the corresponding eigenvalue λ_s is given by Eq. (S123), and the normalization constant is

$$\Lambda_s = \left| \frac{\left(1 - \lambda_s^2\right)}{\sqrt{\lambda_s^4 + \eta^2 - \lambda_s^2 + 4\lambda_s \eta \cos\theta + \lambda_s^2 \eta^2 + 2}} \right|, \qquad s = 1, 2, 3. \tag{S128}$$

When one of these eigenstates is a dark state, then the probability amplitude of the excited state $|e\rangle$ in this eigenstate (S127) is zero, and we have the relation

$$\lambda = -\eta e^{i\theta}. \tag{S129}$$

By substituting the above relation into the secular equation Eq. (S122), we have

$$\eta^3 \left(-e^{i3\theta} + e^{i\theta}\right) + i2\eta \sin\theta = 0, \tag{S130}$$

which leads to these two equations

$$\left[\cos\theta - \cos(3\theta)\right]\eta^3 = 0, \qquad \eta^3 \left[\sin\theta - \sin(3\theta)\right] + 2\eta \sin\theta = 0. \tag{S131}$$

For a nonzero η, the solutions of these two equations are

$$\theta = n\pi, \qquad n = 0, \pm 1, \pm 2, \cdots. \tag{S132}$$

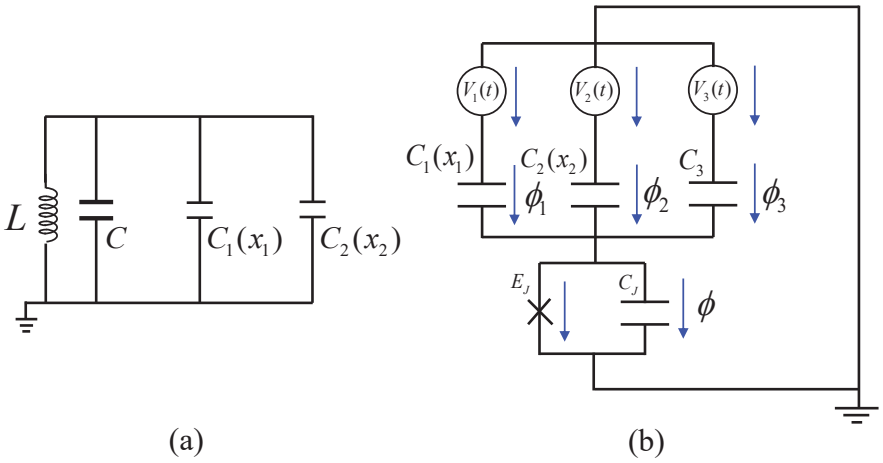

FIG. S16: (a) The circuit electromechanical system consists of a microwave cavity represented by an inductance L and three capacitances: C and $C_{j=1,2}(x_j)$. Here, the two capacitances $C_{j=1,2}(x_j)$ depend on the two micromechanical resonators $b_{j=1,2}$. The displacement $x_{j=1,2}$ of each mechanical resonator modulates the total capacitance and hence the cavity frequency ω_c. A phase-dependent phonon-hopping interaction $\eta(e^{i\theta}b_1^\dagger b_2 + e^{-i\theta}b_2^\dagger b_1)$ between the two micromechanical resonators is generated via a superconducting quantum circuit given in panel (b). (b) Schematic diagram of the superconducting quantum circuit: A Josephson junction with the Josephson energy E_J and the capacitance C_J is connected to three gate voltages $V_{j=1,2,3}(t)$ through the corresponding gate capacitances $C_{j=1,2}(x_j)$ and C_3. Two mechanical resonators are coupled to the superconducting charge qubit through the gate capacitances $C_{j=1,2}(x_j)$. The gate voltages are properly designed such that a phase-dependent phonon-hopping interaction between the two mechanical resonators can be induced. The phase drops across these capacitor $C_{j=1,2,3}$ and the Josephson junction are marked as ϕ_j and ϕ, respectively.

When $\theta = n\pi$, we have $e^{i\theta} = e^{-i\theta} = (-1)^n$, then the eigenvalues of the matrix (S120) are given by

$$\lambda_1 = (-1)^{n+1}\eta, \qquad \lambda_2 = \frac{1}{2}\left[(-1)^n\eta - \sqrt{8+\eta^2}\right], \qquad \lambda_3 = \frac{1}{2}\left[(-1)^n\eta + \sqrt{8+\eta^2}\right]. \tag{S133}$$

The corresponding eigenstates are given by

$$\begin{aligned}
|\lambda_1\rangle &= \frac{1}{\sqrt{2}}(-|f\rangle + |g\rangle), \\
|\lambda_2\rangle &= \Lambda_2\left\{\frac{1}{2}\left[(-1)^{n+1}\eta - \sqrt{8+\eta^2}\right]|e\rangle + |f\rangle + |g\rangle\right\}, \\
|\lambda_3\rangle &= \Lambda_3\left\{\frac{1}{2}\left[(-1)^{n+1}\eta + \sqrt{8+\eta^2}\right]|e\rangle + |f\rangle + |g\rangle\right\},
\end{aligned} \tag{S134}$$

where $\Lambda_{2,3} = [\frac{1}{4}(\sqrt{8+\eta^2} \pm (-1)^n\eta)^2 + 2]^{-1/2}$ are normalization constants. In this case, the eigenstate $|\lambda_1\rangle$ is a dark state.

X. A POSSIBLE EXPERIMENTAL REALIZATION AND DERIVATION OF A PHASE-DEPENDENT PHONON-HOPPING INTERACTION BETWEEN TWO MECHANICAL RESONATORS

A. A possible experimental realization

In this section, we propose a possible experimental implementation of our scheme based on the circuit electromechanical system, as shown in Fig. S16(a). The circuit electromechanical system [S3, S4] consists of a microwave cavity described by the equivalent inductance L and capacitance C and two micromechanical resonators $b_{j=1,2}$. The electromechanical coupling arises when the displacement $x_{j=1,2}$ of each mechanical resonator independently modulates the total capacitance through $C_{j=1,2}(x_j)$, and therefore the resonance frequency of the cavity ω_c. This electromechanical coupling can be described by $g_j = (\omega_c/2C)\partial C_j/\partial x_j$. Meanwhile, an effective phase-dependent phonon-hopping

interaction between the two mechanical resonators is introduced by coupling them to a superconducting charge qubit, as shown in Fig. S16(b). The detailed derivation of the phase-dependent phonon-exchange interaction is presented in the next subsection.

B. Derivation of a phase-dependent phonon-hopping interaction between two mechanical resonators

In this section, we present a detailed derivation of an effective phase-dependent phonon-hopping interaction between two mechanical resonators. Here the two mechanical resonators are coupled to a superconducting charge qubit, which is described by the circuit given in Fig. S16(b). In this circuit, a Josephson junction with the Josephson energy E_J and the capacitance C_J is connected to three gate voltages $V_{j=1,2,3}(t)$ through the corresponding gate capacitances $C_{j=1,2}(x_j)$ and C_3. Here the two gate capacitors with capacitances $C_{j=1,2}(x_j)$ are formed by one fixed plate and one mechanical resonator. The third capacitor has a constant capacitance. We denote the phase drops across these capacitor $C_{j=1,2,3}$ and the Josephson junction as ϕ_j and ϕ, respectively. In this circuit, the energy stored in these capacitors is the total kinetic energy [S5], which can be written as

$$T=\frac{1}{2}C_1(x_1)\dot{\Phi}_1^2+\frac{1}{2}C_2(x_2)\dot{\Phi}_2^2+\frac{1}{2}C_3\dot{\Phi}_3^2+\frac{1}{2}C_J\dot{\Phi}^2, \tag{S135}$$

where $\Phi_{j=1,2,3}$ and Φ are the generalized magnetic fluxes associated with the phase drops ϕ_j and ϕ across the capacitances C_j and the Josephson junction. The relation between the generalized magnetic flux and the phase drop is defined by $\phi_{j=1,2,3}=2\pi\Phi_j/\Phi_0$, where Φ_0 is the magnetic flux quanta. The Josephson energy is identified as the potential energy, which takes the form as [S5]

$$U=-E_J\cos\left(\frac{2\pi}{\Phi_0}\Phi\right), \tag{S136}$$

where E_J is the Josephson energy of this junction.

Based on these voltages relations in these loops, we have the relations

$$V_j(t)+\dot{\Phi}_j+\dot{\Phi} \;=\; 0, \qquad j=1,2,3, \tag{S137}$$

then the Lagrangian of this system can be expressed as

$$\begin{aligned} L &= T-U \\ &= \frac{1}{2}C_1\left(x_1\right)V_1^2\left(t\right)+\frac{1}{2}C_2\left(x_2\right)V_2^2\left(t\right)+\frac{1}{2}C_3V_3^2\left(t\right)+\frac{1}{2}\left(C_1\left(x_1\right)+C_2\left(x_2\right)+C_3+C_J\right)\dot{\Phi}^2 \\ &\quad+\left[C_1\left(x_1\right)V_1\left(t\right)+C_2\left(x_2\right)V_2\left(t\right)+C_3V_3\left(t\right)\right]\dot{\Phi}+E_J\cos\left(\frac{2\pi}{\Phi_0}\Phi\right). \end{aligned} \tag{S138}$$

We introduce the momentum canonically conjugate to Φ as

$$P \;=\; \frac{\partial L}{\partial\dot{\Phi}}=\left[C_1\left(x_1\right)V_1\left(t\right)+C_2\left(x_2\right)V_2\left(t\right)+C_3V_3\left(t\right)\right]+\left[C_1\left(x_1\right)+C_2\left(x_2\right)+C_3+C_J\right]\dot{\Phi}. \tag{S139}$$

Then the Hamiltonian of this circuit can be derived as [S5]

$$\begin{aligned} H &= \frac{1}{2}\frac{4e^2}{C_\Sigma\left(x_1,x_2\right)}\left[\hat{n}-n_g\left(x_1,x_2,t\right)\right]^2-E_J\cos\left(\frac{2\pi}{\Phi_0}\Phi\right) \\ &\quad-\frac{1}{2}\left[C_1\left(x_1\right)V_1^2\left(t\right)+C_2\left(x_2\right)V_2^2\left(t\right)+C_3V_3^2\left(t\right)\right], \end{aligned} \tag{S140}$$

where we introduce the Cooper-pair number n, the gate capacitance $C_\Sigma\left(x_1,x_1\right)$, and the gate Cooper-pair number n_g, which are defined by

$$P=2en, \qquad C_\Sigma\left(x_1,x_2\right)=C_1\left(x_1\right)+C_2\left(x_2\right)+C_3+C_J, \tag{S141}$$

and

$$n_g\left(x_1,x_2,t\right)=\frac{1}{2e}\left[C_1\left(x_1\right)V_1\left(t\right)+C_2\left(x_2\right)V_2\left(t\right)+C_3V_3\left(t\right)\right]. \tag{S142}$$

The quantization of this circuit can be performed by introducing the commutative relation between the number operator $\hat{n}$ and the phase operator $\hat{\phi}$ as $[\hat{\phi},\hat{n}]=i$. Then we can express the Hamiltonian in the eigen-representation of the number operator as

$$\begin{aligned} H &= \frac{1}{2}\frac{4e^2}{C_\Sigma\left(x_1,x_2\right)}\sum_{n\in Z}\left[n-n_g\left(x_1,x_2,t\right)\right]^2|n\rangle\langle n| - \frac{E_J}{2}\sum_{n\in Z}\left(|n\rangle\langle n+1| + |n+1\rangle\langle n|\right) \\ &\quad -\frac{1}{2}\left[C_1\left(x_1\right)V_1^2\left(t\right)+C_2\left(x_2\right)V_2^2\left(t\right)+C_3V_3^2\left(t\right)\right]. \end{aligned} \tag{S143}$$

In this work, we consider the case where this circuit works in the charge qubit regime $E_C \gg E_J$, with $E_C = 4e^2/C_\Sigma$ being the Coulomb energy. In particular, we choose the gate charge in the vicinity of $1/2$, so that the states $|0\rangle$ and $|1\rangle$ have almost degenerate energies. In this case, other states have higher energies and can be ignored in the our discussions. Then the Hamiltonian becomes

$$\begin{aligned} H &\approx \frac{1}{2}\frac{4e^2}{C_\Sigma\left(x_1,x_2\right)}\left[n_g\left(x_1,x_2,t\right)^2|0\rangle\langle 0| + \left[1-n_g\left(x_1,x_2,t\right)\right]^2|1\rangle\langle 1|\right] - \frac{E_J}{2}\left(|0\rangle\langle 1| + |1\rangle\langle 0|\right) \\ &\quad -\frac{1}{2}\left[C_1\left(x_1\right)V_1^2\left(t\right)+C_2\left(x_2\right)V_2^2\left(t\right)+C_3V_3^2\left(t\right)\right]. \end{aligned} \tag{S144}$$

By introducing the Pauli operators $|0\rangle\langle 0| - |1\rangle\langle 1| = \sigma_z$ and $|0\rangle\langle 0| + |1\rangle\langle 1| = I$, we can express the Hamiltonian as

$$H = \frac{1}{2}\frac{4e^2}{C_\Sigma\left(x_1,x_2\right)}\left[n_g\left(x_1,x_2,t\right)-\frac{1}{2}\right]\sigma_z - \frac{E_J}{2}\sigma_x + M, \tag{S145}$$

where the term M stands for the ac voltage driving term on these two mechanical resonators

$$M = \frac{1}{4}\frac{4e^2}{C_\Sigma\left(x_1,x_2\right)}\left[1-2n_g\left(x_1,x_2,t\right)+2n_g^2\left(x_1,x_2,t\right)\right] - \frac{1}{2}\left[C_1\left(x_1\right)V_1^2\left(t\right)+C_2\left(x_2\right)V_2^2\left(t\right)+C_3V_3^2\left(t\right)\right]. \tag{S146}$$

We consider the case in which the voltage drivings are far-off-resonance to these two mechanical resonators (namely the driving frequencies of the two voltages are much smaller than the resonance frequencies of the two mechanical resonators) and then the term M will be discarded in our following discussions. When the vibration amplitudes of the mechanical resonators are much smaller than the distances between the fixed plate and the rest mechanical resonator of the capacitors, we can approximate the capacitances as

$$C_1\left(x_1\right) \approx C_{10}\left(1-\frac{x_1}{l_1}\right), \qquad C_2\left(x_2\right) \approx C_{20}\left(1-\frac{x_2}{l_2}\right), \tag{S147}$$

where C_{j0} (for $j=1,2$) are the capacitances of the gate capacitors when the mechanical resonators are rest, and $l_{j=1,2}$ are the rest distances between the fixed plate and the mechanical resonators in these gate capacitors. In addition, we choose the following gate voltages for our purpose,

$$V_1\left(t\right) = V_{10}\cos\left(\omega_1 t+\varphi_1\right), \qquad V_2\left(t\right) = V_{20}\cos\left(\omega_2 t+\varphi_2\right), \qquad V_3\left(t\right) = \frac{e-C_{10}V_1(t)-C_{20}V_2(t)}{C_3}. \tag{S148}$$

In this case, we can obtain the relation

$$n_g\left(x_1,x_2,t\right)-\frac{1}{2} = -\left[\frac{C_{10}V_{10}}{2e}\frac{x_1}{l_1}\cos\left(\omega_1 t+\varphi_1\right) + \frac{C_{20}V_{20}}{2e}\frac{x_2}{l_2}\cos\left(\omega_2 t+\varphi_2\right)\right]. \tag{S149}$$

By making the rotation for the qubit $-\sigma_x \to \tau_z$ and $\sigma_z \to \tau_x$, we can express the Hamiltonian upto the first order of the mechanical displacements x_1 and x_2 as

$$H_I \approx \frac{E_J}{2}\tau_z - \frac{E_C}{2}\left[\frac{C_{10}V_{10}}{2e}\frac{x_1}{l_1}\cos\left(\omega_1 t+\varphi_1\right) + \frac{C_{20}V_{20}}{2e}\frac{x_2}{l_2}\cos\left(\omega_2 t+\varphi_2\right)\right]\tau_x, \tag{S150}$$

where $E_C = 4e^2/C_{\Sigma 0}$ under the approximation $C_\Sigma\left(x_1,x_2\right) \approx \left(C_{10}+C_{20}+C_J\right) \equiv C_{\Sigma 0}$. We should point out that the mechanical displacement terms in $C_\Sigma\left(x_1,x_2\right)$ only introduce the second-order terms of $x_{j=1,2}/l_j$, which have been neglected in our considerations.

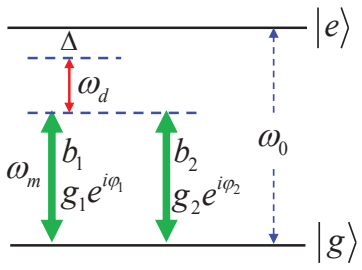

FIG. S17: Schematic diagram of the energy levels and these involved resonance frequencies of this coupled qubit-resonator system. Two mechanical resonators with resonance frequency ω_m are phase-dependently coupled to the superconducting charge qubit with the energy separation ω_0. The ac gate voltages with frequency ω_d are applied to the Josephson junction through the gate capacitors.

By including the free Hamiltonian of the two mechanical resonators and using the relations $x_{j=1,2} = \sqrt{\hbar/(2m\omega_m)}(b_j + b_j^\dagger)$ and $p_{j=1,2} = -i\sqrt{\hbar m\omega_m/2}(b_j - b_j^\dagger)$, the total Hamiltonian of this circuit system becomes

$$\begin{aligned} H_I \;\approx\; & \omega_m b_1^\dagger b_1 + \omega_m b_2^\dagger b_2 + \frac{\omega_0}{2}\tau_z \\ & - \left[g_1\left(b_1 + b_1^\dagger\right)\left(e^{i(\omega_d t+\varphi_1)} + e^{-i(\omega_d t+\varphi_1)}\right) + g_2\left(b_2 + b_2^\dagger\right)\left(e^{i(\omega_d t+\varphi_2)} + e^{-i(\omega_d t+\varphi_2)}\right)\right](\tau_+ + \tau_-), \end{aligned} \tag{S151}$$

where we consider the case $\omega_1 = \omega_2 = \omega_d$ and introduce these parameters

$$g_1 = \frac{E_C}{4}\frac{C_{10}V_{10}}{2e}\frac{x_{10}}{l_1}, \qquad g_2 = \frac{E_C}{4}\frac{C_{20}V_{20}}{2e}\frac{x_{20}}{l_2}, \qquad \omega_0 = E_J, \tag{S152}$$

with $x_{j0} = \sqrt{\hbar/(2m\omega_m)}$ being the zero-point fluctuation of these mechanical resonators.

To analyze the physical processes in this system, we now work in the rotating frame with respect to

$$H_0 = \omega_m b_1^\dagger b_1 + \omega_m b_2^\dagger b_2 + \frac{\omega_0}{2}\tau_z, \tag{S153}$$

then the Hamiltonian becomes

$$\begin{aligned} V_I(t) \;=\; & -g_1(\tau_+ b_1^\dagger e^{i(\omega_0+\omega_m+\omega_d)t}e^{i\varphi_1} + b_1\tau_- e^{-i(\omega_0+\omega_m+\omega_d)t}e^{-i\varphi_1}) \\ & -g_2(\tau_+ b_2^\dagger e^{i(\omega_0+\omega_m+\omega_d)t}e^{i\varphi_2} + b_2\tau_- e^{-i(\omega_0+\omega_m+\omega_d)t}e^{-i\varphi_2}) \\ & -g_1(\tau_+ b_1^\dagger e^{i(\omega_0+\omega_m-\omega_d)t}e^{-i\varphi_1} + b_1\tau_- e^{-i(\omega_0+\omega_m-\omega_d)t}e^{i\varphi_1}) \\ & -g_2(\tau_+ b_2^\dagger e^{i(\omega_0+\omega_m-\omega_d)t}e^{-i\varphi_2} + b_2\tau_- e^{-i(\omega_0+\omega_m-\omega_d)t}e^{i\varphi_2}) \\ & -g_1(\tau_+ b_1 e^{i(\omega_0-\omega_m+\omega_d)t}e^{i\varphi_1} + b_1^\dagger\tau_- e^{-i(\omega_0-\omega_m+\omega_d)t}e^{-i\varphi_1}) \\ & -g_2(\tau_+ b_2 e^{i(\omega_0-\omega_m+\omega_d)t}e^{i\varphi_2} + b_2^\dagger\tau_- e^{-i(\omega_0-\omega_m+\omega_d)t}e^{-i\varphi_2}) \\ & -g_1(\tau_+ b_1 e^{i(\omega_0-\omega_m-\omega_d)t}e^{-i\varphi_1} + b_1^\dagger\tau_- e^{-i(\omega_0-\omega_m-\omega_d)t}e^{i\varphi_1}) \\ & -g_2(\tau_+ b_2 e^{i(\omega_0-\omega_m-\omega_d)t}e^{-i\varphi_2} + b_2^\dagger\tau_- e^{-i(\omega_0-\omega_m-\omega_d)t}e^{i\varphi_2}). \end{aligned} \tag{S154}$$

Here we can see that in this system there are eight physical processes, which are determined by the four detunings $\omega_0+\omega_m\pm\omega_d$ and $\omega_0-\omega_m\pm\omega_d$. From the viewpoint of the qubit and the resonators, the terms including $\omega_0+\omega_m\pm\omega_d$ and $\omega_0-\omega_m\pm\omega_d$ are the counterrotating terms and the corotating terms, respectively. In this work, the motivation for introducing the ac voltages $V_1(t)$ and $V_2(t)$ is to pick up the phase-sensitive interactions between the mechanical resonators and the charge qubit. For this purpose, we choose the ac voltages with the frequency ω_d to pick up the terms with $\omega_0 - \omega_m - \omega_d$. Namely, we choose the parameters to satisfy the following parameter conditions

$$\omega_0 + \omega_m \pm \omega_d \gg \omega_0 - \omega_m + \omega_d \gg \omega_0 - \omega_m - \omega_d. \tag{S155}$$

The terms with $\omega_0 + \omega_m \pm \omega_d$ and $\omega_0 - \omega_m + \omega_d$ are the far-off-resonance terms and the terms with $\omega_0 - \omega_m - \omega_d$ are the target terms which work in the large-detuning regime. The energy levels and these involved resonance frequencies of this coupled qubit-resonator system are shown in Fig. S17. In this case, the qubit-resonator interactions

work in the large-detuning regime: $\Delta \gg g_{j=1,2}\sqrt{n_j}$, where n_j is the maximal excitation number involved in the jth mechanical resonator, and then we can obtain a phase-dependent photon-hopping interaction between the two mechanical resonators. Here the phase is the difference between the two phases φ_1 and φ_2 associated with the qubit-resonator couplings.

Based on the above analyses, we can obtain the approximate Hamiltonian as

$$V_I(t) \approx -\left[\tau_+\left(g_1 b_1 e^{-i\varphi_1}+g_2 b_2 e^{-i\varphi_2}\right)e^{i\Delta t}+\left(g_1 b_1^\dagger e^{i\varphi_1}+g_2 b_2^\dagger e^{i\varphi_2}\right)\tau_- e^{-i\Delta t}\right], \tag{S156}$$

where we introduce the detuning $\Delta = \omega_0 - \omega_m - \omega_d$. The time factor can be eliminated by going back to the Schrödinger representation, in which the Hamiltonian of the system can be written as

$$H_{\rm eff} = \omega_m b_1^\dagger b_1 + \omega_m b_2^\dagger b_2 + \frac{\omega_0-\omega_d}{2}\tau_z - \tau_+\left(g_1 b_1 e^{-i\varphi_1}+g_2 b_2 e^{-i\varphi_2}\right) - \left(g_1 b_1^\dagger e^{i\varphi_1}+g_2 b_2^\dagger e^{i\varphi_2}\right)\tau_-. \tag{S157}$$

In this work, we consider the physical process associated with the detuning Δ working in the large detuning case. Then we can adiabatically eliminate the qubit coherence in the physical processes and an effective phonon-phonon interaction between the two mechanical modes can be induced by the second-order perturbation. In this case, we can derive an effective Hamiltonian to describe the interactions using the method of the Frohlich-Nakajima transformation [S6, S7]. To this end, we express the effective Hamiltonian $H_{\rm eff}$ as two parts

$$\begin{aligned} H_0 &= \omega_m b_1^\dagger b_1 + \omega_m b_2^\dagger b_2 + \frac{\omega_0-\omega_d}{2}\tau_z, \\ H_I &= -\tau_+\left(g_1 b_1 e^{-i\varphi_1}+g_2 b_2 e^{-i\varphi_2}\right) - \tau_-\left(g_1 b_1^\dagger e^{i\varphi_1}+g_2 b_2^\dagger e^{i\varphi_2}\right). \end{aligned} \tag{S158}$$

We also introduce the operator

$$S = \frac{1}{\Delta}\tau_+\left(g_1 b_1 e^{-i\varphi_1}+g_2 b_2 e^{-i\varphi_2}\right) - \frac{1}{\Delta}\left(g_1 b_1^\dagger e^{i\varphi_1}+g_2 b_2^\dagger e^{i\varphi_2}\right)\tau_-, \tag{S159}$$

which is determined by the equation

$$H_I + [H_0, S] = 0. \tag{S160}$$

This equation means that the first-order physical process is eliminated. An effective Hamiltonian describing the second-order physical interaction can then be obtained as

$$\begin{aligned} H'_{\rm eff} &= H_0 + \frac{1}{2}[H_I, S] \\ &= \omega_m b_1^\dagger b_1 + \omega_m b_2^\dagger b_2 + \frac{\omega_0-\omega_d}{2}\tau_z + \frac{g_1^2}{\Delta}\tau_z b_1^\dagger b_1 + \frac{g_2^2}{\Delta}\tau_z b_2^\dagger b_2 + \frac{\left(g_1^2+g_2^2\right)}{\Delta}\tau_+\tau_- \\ &\quad + \frac{g_1 g_2}{\Delta}\tau_z\left(b_1^\dagger b_2 e^{i(\varphi_1-\varphi_2)} + b_2^\dagger b_1 e^{-i(\varphi_1-\varphi_2)}\right). \end{aligned} \tag{S161}$$

The above Hamiltonian shows that there is no transition in the qubit states, and that a conditional phase-dependent interaction between the two mechanical resonators is introduced. We assume that the qubit is initial in its ground state $|g\rangle$ ($\tau_z|g\rangle = -|g\rangle$), then a phase-dependent phonon-hopping interaction is obtained.

[S1] D. Ramos, I. W. Frank, P. B. Deotare, I. Bulu, and M. Lončar, Non-linear mixing in coupled photonic crystal nanobeam cavities due to cross-coupling opto-mechanical mechanisms, App. Phys. Lett. **105**, 181121 (2014).

[S2] Y.-x. Liu, J. Q. You, L. F. Wei, C. P. Sun, and F. Nori, Optical Selection Rules and Phase-Dependent Adiabatic State Control in a Superconducting Quantum Circuit, Phys. Rev. Lett. **95**, 087001 (2005).

[S3] F. Massel, T. T. Heikkilä, J.-M. Pirkkalainen, S. U. Cho, H. Saloniemi, P. J. Hakonen, and M. A. Sillanpää, Microwave amplification with nanomechanical resonators, Nature (London) **480**, 351 (2011).

[S4] F. Massel, S. U. Cho, J.-M. Pirkkalainen, P. J. Hakonen, T. T. Heikkilä, and M. A. Sillanpää, Multimode circuit optomechanics near the quantum limit, Nat. Commun. **3**, 987 (2012).

[S5] M. Nakahara and T. Ohmi, *Quantum Computing: From Linear Algebra to Physical Realizations* (CRC Press, Boca Raton, 2008).

[S6] H. Fröhlich, Phys. Rev. **79**, 845 (1950).

[S7] S. Nakajima, Adv. Phys. **4**, 463 (1953).